ANALYSIS OF FRAME STRUCTURES MADE OF LINEAR VISCOELASTIC MATERIALS

Thesis for the Degree of Ph. D.

MICHIGAN STATE UNIVERSITY

MARK M. BERRIO

1970

This is to certify that the

thesis entitled

ANALYSIS OF FRAME STRUCTURES MADE OF LINEAR VISCOELASTIC MATERIALS

presented by

Mark M. Berrio

has been accepted towards fulfillment
of the requirements for

Ph. D. degree in Civil Engineering

O. E. Cutts

Major professor

Date Dec 1, 1970

6 — 188

ABSTRACT

ANALYSIS OF FRAME STRUCTURES MADE OF
LINEAR VISCOELASTIC MATERIALS

By

Mark M. Berrio

A matrix formulation method is presented for the analysis of plane frame structures made of linear viscoelastic materials. The study will follow the isothermal quasi-static linear theory of homogeneous viscoelastic solids. Geometric non-linearity and effect of axial forces on the flexural stiffness of the members is taken into consideration.

A computer program written in FORTRAN is prepared for the implementation of the analysis. Three numerical examples are considered, and the results are compared with those obtained from experimental work.

The method is based on the calculation of a fictitious load vector, obtained from the structure's deformation history and added to the actual external load vector as time increases. The computation of the fictitious load vector is carried out by a finite difference method scheme.

Mark M. Berrio

Creep tests are run to establish the viscoelastic properties of the material experimentally, rather than using spring dashpot models. A direct numerical inversion is then carried out, yielding the relaxation modulus values without resorting to the use of the Laplace transform.

ANALYSIS OF FRAME STRUCTURES MADE OF LINEAR VISCOELASTIC MATERIALS

By

Mark M. Berrio

A THESIS

Submitted to
Michigan State University
in partial fulfillment of the requirements
for the degree of

DOCTOR OF PHILOSOPHY

Department of Civil Engineering

1970

ACKNOWLEDGMENTS

The writer would like to express his appreciation to Michigan State University, and to his guidance committee Dr. Charles E. Cutts, chairman, Dr. George E. LaPalm, Dr. James L. Lubkin, Dr. George E. Mase and Dr. David H. Y. Yen for their support and assistance.

The writer is especially grateful to Dr. George E. LaPalm, who as major professor provided direction and encouragement throughout the course of his study.

A special word of thanks is extended to the writer's wife, Margaret, for her help in the laboratory work, for her typing of the rough draft, and above all for her patience and understanding during these three years at Michigan State University.

TABLE OF CONTENTS

LIST OF TABLES

LIST OF CHARTS

LIST OF FIGURES

CHAPTER I

INTRODUCTION

1.1 Viscoelastic Materials

Although the origins of the theory of viscoelasticity can be traced to isolated cases during the second half of the nineteenth century, it has not been until recent years that the subject has received close attention.

Time dependent deformation or creep, as it is commonly named, arises in a number of modern structural situations. High temperatures induce material inelasticity, loss of strength and stiffness, creep, etc. Asphalt pavements and solid fuel in rockets offer two more instances of engineering applications of viscoelastic materials.

However, it is due largely to the recent advances in highpolymer technology that the theory of viscoelasticity has attracted an ever-growing interest.

1.2 Previous Work

Recent investigations in linear viscoelasticity may be divided into two general groups. The first group is concerned with the basic constitutive equations, and deals with the subject from the viewpoint of continuum mechanics. The second group is concerned with the solution of

boundary value problems, with a number of solutions to particular problems.

In 1954, Hoff (11)* proved that, for a body subject to stationary creep under the action of constant forces, it is always possible to use an elastic analogue. Here by state of stationary creep is meant one where the space distribution of stress in the body remains constant. The elastic analogy has been used by Hult (12), Patel and Venkatraman (15), Odqvist (14), and others, in the analysis of trusses, beams and plates. Williams (19) carried out a structural analysis using spring dashpot mechanical models to represent the viscoelastic materials. Flügge (5) solves the beam problem by means of the correspondence principle, which links the linear theories of viscoelasticity and elasticity.

The correspondence principle can be stated in a general form saying that, if the solution of an elastic problem is known, the Laplace transform of the solution of the corresponding viscoelastic problem may be found by an appropriate replacement of the elastic constants by viscoelastic operator polynomials, and the actual loads by their Laplace transforms (5).

The writer recognizes that this is hardly a comprehensive review of the recent work on viscoelasticity.

---

*Numerals with no punctuation in parentheses refer to entries in the list of references.

The list of papers could go on showing a number of solutions to beam, bars, plates and columns, based on spring dashpot models, differential operators, Laplace transform, etc. As it has been pointed out, most of the investigation on linear viscoelasticity has been done from a continuum mechanics or applied mathematics point of view, and, therefore, somewhat different from the framed structure analysis in which we are interested in this study.

1.3 Objective and Outline of This Work

LaPalm (13) developed a numerical integration scheme which allowed him to write lower and upper bounds to the solution of the governing equation of a linear viscoelastic beam-column. The objective of this study will be the development of a practical computer matrix method for the analysis of linear viscoelastic frames, using LaPalm's results as a basis and point of departure.

Creep tests will be conducted to establish the material's properties experimentally, rather than using spring dashpot mechanical models. In Chapter II an inversion of the creep compliance values will be performed, yielding the relaxation modulus values. A computer program will be written for this purpose, again making use of results obtained by LaPalm (13).

Chapter III will provide the results needed to write a computer program to carry out the analysis of framed

structures made of viscoelastic materials. This will constitute the main goal of this study.

The laboratory investigation will be presented in Chapter IV. Several creep tests will be run to establish the viscoelastic properties of the material. Rigid two-dimensional frames will be tested under constant joint loads.

The theoretical and laboratory results will be presented and compared in Chapter V.

Finally, a brief summary with conclusions will be given in Chapter VI.

Notation and listing of computer programs will be included in Appendices A and B, respectively.

1.4 Assumptions and Limitations

Effects of changes in temperature, and temperature gradient will be excluded from this study, i.e., the structure will be considered at a uniform constant temperature, free of thermal stresses.* The inertia term is considered small, and therefore dropped from the equation of motion (quasi-static case).

The study will be restricted to the viscoelastic linear range of the material. For the creep tests, the space distribution of stress in the body will be considered to remain constant, giving rise to a state of stationary creep.

---

*The test room was kept at all times at a virtually constant temperature of 80.5°F.

The assumption of plane sections remaining plane after bending will be used here. Equilibrium will be enforced in accordance with the geometry of the deformed structure. Finally, the effect of axial forces on the flexural stiffness of the members will be taken into consideration.

CHAPTER II

CREEP COMPLIANCE INVERSION

2.1 Some Definitions

The creep compliance, $D(t)$, of a viscoelastic material can be defined as the strain, varying with time, due to a unit constant stress. If $\varepsilon(t)$ represents the strain as a function of time, and σ_o the constant unit stress, we can write

$$\varepsilon(t) = D(t)\sigma_o \tag{2.1}$$

The creep compliance is a property of the material related to its internal constitution. In the case of high polymers the orientation of crystals will have its effect in the creep compliance of the material (1) (3).

The creep compliance is a monotonically increasing function for all $t>0$ (4). For high polymers, the rate at which $D(t)$ increases diminishes with time, approaching zero as time approaches infinity (3).

Equation (2.1) shows that discrete values of $D(t)$ can be obtained readily by measuring the deformations, $\Delta(t)$, that will occur when the material is kept under constant load. See Chapter IV for a full description of

the way in which values of D(t) were obtained for the models used in this work.

Some numerical formulations of problem solutions are more easily handled using the so-called relaxation modulus, E(t), which can be defined as the stress varying with time due to a constant unit strain. Letting $\sigma(t)$ be the stress as a function of time, and ε_o be the constant unit strain, we can write

$$\sigma(t) = E(t)\ \varepsilon_o \qquad (2.2)$$

The relaxation modulus is monotonically decreasing (4). For details about the relaxation modulus and the internal constitution of materials such as high polymers, the reader is referred again to references (1) and (3).

It will be shown in Chapter III that correspondence can be established between the role of the relaxation modulus in the analysis of viscoelastic structures, and that of the modulus of elasticity in the analysis of elastic structures. Due to this circumstance, it will be preferable to work with the relaxation modulus, rather than with the creep compliance. This resolves, in some way, the viscoelastic problem into a succession of elastic solutions.

It can be seen from Equation (2.2), that by inducing a constant unit strain, ε_o, and measuring the resulting stress

$\sigma(t)$, as a function of time, a direct numerical evaluation of $E(t)$ is possible. This is known as the relaxation test. In a relaxation test, a displacement is induced and kept constant. Then the force is measured as it varies with time. The crux of the problem lies in the fact that forces are read by measuring displacements. In essence, one is supposed to measure the displacements which are occurring while holding the displacement constant. This would require more time and more sophisticated equipment than were available for the present study.

This is why creep tests were run, as will be seen in Chapter IV. From the creep compliance values, the sought relaxation modulus values were obtained, as will be shown later in this chapter.

2.2 Relation Between Creep Compliance and Relaxation Modulus

The Laplace transforms of the creep compliance, $\bar{D}(s)$, and relaxation modulus, $\bar{E}(s)$, are related by the simple expression

$$\bar{D}(s)\ \bar{E}(s) = \frac{1}{s^2} \tag{2.3}$$

A rigorous proof of Equation (2.3) is offered by Gurtin and Sternberg (9) in the form of a theorem. The same relation is derived in a simpler way by a number of writers, e.g., Fung (7). Equation (2.3) is well known in

viscoelasticity, and what we propose to do is to carry out an actual numerical inversion, i.e., given a set of values of D(t), find the corresponding numerical values of E(t).

The usefulness of a direct application of Equation (2.3) will depend on the forms of $\bar{E}(s)$ and $\bar{D}(s)$. For a simple spring-dash model the inversion will be readily performed. When a set of laboratory data for a real viscoelastic material is the only information available, a direct application of Equation (2.3) is impossible, and a numerical scheme has been devised to make the inversion practical.

2.3 Upper and Lower Bounds for the Relaxation Modulus

In reference (13) it is formally shown that an approximation as to what might be considered as upper and lower bounds to the true values of E(t) are given by the following two expressions

$$E(t_k) \leq \frac{1 - \sum_{i=2}^{k} E(t_k - t_{i-1}) \left[D(t_i) - D(t_{i-1})\right]}{D(t_1)} \tag{2.4}$$

$$E(t_k) \geq \frac{1 - \sum_{i=1}^{k} E(t_k - t_i) \left[D(t_i) - D(t_{i-1})\right]}{D(0)} \tag{2.5}$$

where E(t) refers to the value of E(t) at time t_k. The finite intervals of time t_1, t_2,..., t_i,..., t_{k-1}, t_k need not be equal.

For the sake of completeness, and in order to establish a more objective basis for the value to be assigned to the expressions (2.4) and (2.5), a development of such expressions follows. This deduction parallels a similar one in reference (13), Appendix B.

Applying the convolution theorem to Equation (2.3), the following expressions are formally obtained:

$$E(t)\ D(0) + \int_0^t E(t-\tau)\ \frac{d}{d\tau}\ D(\tau)\ d\tau = 1 \qquad (2.6)$$

$$D(t)\ E(0) + \int_0^t D(t-\tau)\ \frac{d}{d\tau}\ E(\tau)\ d\tau = 1 \qquad (2.7)$$

The same results are stated and proved by Gurtin and Sternberg (9).

Except at time equal to zero where the relaxation modulus E(t) has a singularity (7), E(t) is a well behaved smooth function, so that one can write:

$$\int_0^{t_k} E(t_k-\tau)\ \frac{d}{d\tau}\ D(\tau)\ d\tau = \sum_{i=1}^{k} \int_{t_{i-1}}^{t_i} E(t_k-\tau)\ \frac{d}{d\tau}\ D(\tau)\ d\tau \qquad (2.8)$$

where $t_o < t_1 < t_2 <...< t_{i-1} < t_i <...< t_{k-1} < t_k$.

Also the following expression can be written

$$\int_{t_{i-1}}^{t_i} E(t_k-\tau)\,\frac{d}{d\tau}D(\tau)\,d\tau = \lim_{\substack{n\to\infty \\ (\Delta\tau_j)_{max}\to 0}} \sum_{j=1}^{n} E(t_k-\tau_j')\,\frac{d}{d\tau}D(\tau_j')\,\Delta\tau_j \tag{2.9}$$

where (see Figure 2.1):

$$t_{i-1} = \tau_o < \tau_1' < \tau_1, \ldots, \tau_{n-1} < \tau_n' < \tau_n = t_i$$

$$\Delta\tau_j = \tau_j - \tau_{j-1}$$

If E(t) decreases monotonically, then

$$E(t_k-\tau_{j-1}) \geq E(t_k-\tau_j') \geq E(t_k-\tau_j) \tag{2.10}$$

$$E(t_k-t_{i-1}) \geq E(t_k-\tau_j') \geq E(t_k-t_i) \tag{2.11}$$

If, in addition, $\frac{d}{d\tau}D(\tau) \geq 0$, letting $\Delta \equiv (\Delta\tau_j)_{max}$, one can write

$$E(t_k-t_{i-1}) \lim_{\substack{n\to\infty \\ \Delta\to 0}} \sum_{j=1}^{n} \frac{d}{d\tau}D(\tau_j')\,\Delta\tau_j \geq$$

$$\geq \lim_{\substack{n\to\infty \\ \Delta\to 0}} \sum_{j=1}^{n} E(t-\tau_j')\,\frac{d}{d\tau}D(\tau_j')\,\Delta\tau \geq$$

$$\geq E(t_k-t_i) \lim_{\substack{n\to\infty \\ \Delta\to 0}} \sum_{j=1}^{n} \frac{d}{d\tau}D(\tau_j')\,\Delta\tau_j \tag{2.12}$$

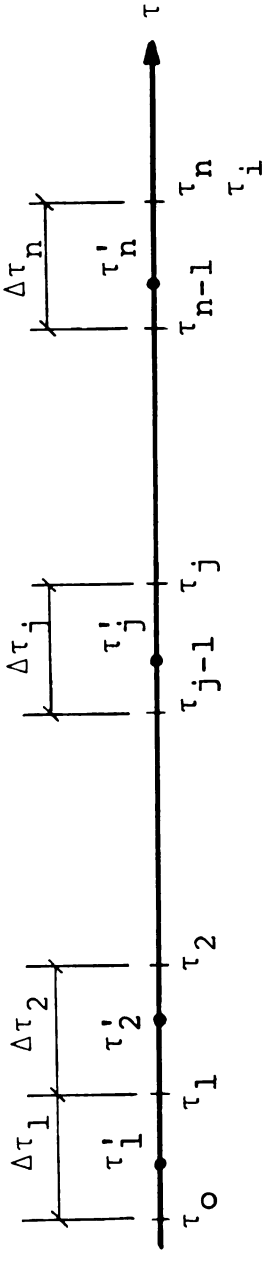

Figure 2.1.--Time intervals.

Combining Equations (2.9) and (2.12), one gets

$$E(t_k-t_{i-1}) \int_{t_{i-1}}^{t_i} \frac{d}{d\tau} D(\tau)\, d\tau \leq \int_{t_{i-1}}^{t_i} E(t_k-\tau) \frac{d}{d\tau} D(\tau)\, d\tau$$

$$\leq E(t_k-t_i) \int_{t_{i-1}}^{t_i} \frac{d}{d\tau} D(\tau)\, d\tau \qquad (2.13)$$

Integrating first and third integrals

$$E(t_k-t_{i-1})[D(t_i) - D(t_{i-1})] \leq \int_{t_{i-1}}^{t_i} E(t_k-\tau) \frac{d}{d\tau} D(\tau)\, d\tau$$

$$\leq E(t_k-t_i)[D(t_i) - D(t_{i-1})] \qquad (2.14)$$

Taking a summation from 1 to k of each member

$$\sum_{i=1}^{k} E(t_k-t_{i-1})[D(t_i)-D(t_{i-1})] \leq \sum_{i=1}^{k} \int_{t_{i-1}}^{t_i} E(t_k-\tau) \frac{d}{d\tau} D(\tau)\, d\tau$$

$$\leq \sum_{i=1}^{k} E(t_k-t_i)[D(t_i)-D(t_{i-1})] \qquad (2.15)$$

Substituting Equation (2.8) in the middle member

$$\sum_{i=1}^{k} E(t_k - t_{i-1})[D(t_i) - D(t_{i-1})] \leq \int_0^{t_k} E(t_k - \tau) \frac{d}{d\tau} D(\tau)\, d\tau$$

$$\leq \sum_{i=1}^{k} E(t_k - t_i)[D(t_i) - D(t_{i-1})] \qquad (2.16)$$

Adding $E(t)D(o)$ to the three members of the above inequality, and substituting the value of Equation (2.6), we get the following two inequalities:

$$E(t_k)D(o) + \sum_{i=1}^{k} E(t_k - t_{i-1})[D(t_i) - D(t_{i-1})] \leq 1 \qquad (2.17)$$

$$E(t_k)D(o) + \sum_{i=1}^{k} E(t_k - t_i)[D(t_i) - D(t_{i-1})] \leq 1 \qquad (2.18)$$

Taking the first term out of the summation, and transposing, one gets from the Equation (2.17)

$$E(t_k)D(o) + E(t_k)[D(t_1) - D(O)]$$

$$\leq 1 - \sum_{i=2}^{k} E(t_k - t_{i-1})[D(t_i) - D(t_{i-1})] \qquad (2.19)$$

$$E(t_k)D(o) + E(t_k)D(t_1) - E(t_k)D(o)$$

$$\leq 1 - \sum_{i=2}^{k} E(t_k - t_{i-1})[D(t_i) - D(t_{i-1})] \qquad (2.20)$$

Finally, cancelling and transposing, Equations (2.4) and (2.5) are obtained. This development, although somewhat detailed, should be considered heuristic, rather than as a rigorous establishment of Equations (2.4) and (2.5). Therefore, a test of the validity of these two equations as upper and lower bounds, respectively, follows.

At time $t_k = t_1$, Equation (2.4) may be written as

$$E_U(t_1) = \frac{1}{D(t_1)} \tag{2.21}$$

Here the subscript U has been introduced to identify $E_U(t_1)$ as the supposed upper bound to the exact value $E(t_1)$ obtained from Equation (2.6) for $t = t_1$, as follows

$$E(t_1)\ D(0) = 1 - \int_0^{t_1} E(t_1 - \tau)\ \frac{d}{d\tau} D(\tau)\ d\tau\ . \tag{2.22}$$

Let $e_U(t_1)$ be defined so that

$$E_U(t_1) = E(t_1) + e_U(t_1). \tag{2.23}$$

Equation (2.21) becomes

$$e_U(t_1)\ D(t_1) = 1 - E(t_1)\ D(t_1) \tag{2.24}$$

Subtracting Equation (2.22) from Equation (2.24) yields

$$e_U(t_1)\ D(t_1) = \int_0^{t_1} E(t_1-\tau)\ \frac{d}{d\tau} D(\tau)\ d\tau - E(t_1)[D(t_1) - D(0)]. \tag{2.25}$$

From Equation (2.16) one can write

$$\int_0^{t_1} E(t_1-\tau)\ \frac{d}{d\tau} D(\tau)\ d\tau \geq E(t_1)\ [D(t_1) - D(0)]. \tag{2.26}$$

Thus

$$e_U(t_1)\ D(t_1) \geq 0 \tag{2.27}$$

and, therefore

$$e_U(t_1) \geq 0 \tag{2.28}$$

which means that $E_U(t_1)$, as given by Equation (2.21), is the upper bound to $E(t_1)$.

At time $t_k = t_n$, Equation (2.4) may be written as

$$E_U(t_n)\ D(t_1) = 1 - \sum_{i=2}^{n} E_U(t_n-t_{i-1})\ [D(t_i) - D(t_{i-1})]. \tag{2.29}$$

Let $e_U(t_n)$ be defined so that

$$E_U(t_n) = E(t_n) + e_U(t_n). \tag{2.30}$$

From Equations (2.29) and (2.30) it follows that

$$e_U(t_n)D(t_1) = 1 - E(t_n)D(t_i) - \sum_{i=2}^{n} E_U(t_n - t_{i-1})[D(t_i) - D(t_{i-1})] \tag{2.31}$$

Equation (2.6) at time $t = t_n$ becomes

$$E(t_n)\ D(0) = 1 - \int_0^{t_n} E(t_n - \tau)\ \frac{d}{d\tau} D(\tau)\ d\tau. \tag{2.32}$$

Subtracting Equation (2.32) from Equation (2.31) yields

$$e_U(t_n)\ D(t_1) = \int_0^{t_n} E(t_n - \tau)\ \frac{d}{d\tau} D(\tau)\ d\tau - E(t_n)\ [D(t_1) - D(0)]$$

$$- \sum_{i=2}^{n} E_U(t_n - t_{i-1})\ [D(t_i) - D(t_{i-1})]. \tag{2.33}$$

Since D(t) is monotonically increasing, it follows that

$$E(t_n)\ [D(t_1) - D(0)] > 0 \tag{2.34}$$

and

$$\sum_{i=2}^{n} E_U(t_n - t_{i-1})\ [D(t_i) - D(t_{i-1})] > 0 \tag{2.35}$$

Also from Equation (2.16) one has

$$\int_{o}^{t_n} E(t_n-\tau)\ \frac{d}{d\tau}\ D(\tau)\ d\tau \geq \sum_{i=1}^{n} E(t_n-t_{i-1})\ [D(t_i) - D(t_{i-1})].$$

(2.36)

Now Equation (2.33) can be transformed into the following inequality

$$e_U(t_n)\ D(t_1) \geq \sum_{i=1}^{n} E(t_n - t_{i-1})\ [D(t_i) - D(t_{i-1})]$$

$$- E(t_n)\ [D(t_1) - D(0)]$$

$$- \sum_{i=2}^{n} E_U(t_n - t_{i-1})\ [D(t_i) - D(t_{i-1})]$$

(2.37)

which can be written in the following form

$$e_U(t_n)\ D(t_1) \geq \sum_{i=2}^{n} [E(t_n-t_{i-1}) - E_U(t_n-t_{i-1})][D(t_i)-D(t_{i-1})].$$

(2.38)

If $E_U(t)$ is greater than $E(t)$ in the above expression, the right-hand side of the inequality will be the product of negative and positive values, and, hence, negative. Therefore no conclusion can be drawn with respect to the sign of $e_U(t_n)$. Hence, the test fails to prove whether or not $E_U(t_n)$ provides the upper bound to $E(t_n)$.

Similarly, at time $t_k = t_1$, Equation (2.5) can be written as

$$E_L(t_1)\ D(0) = 1 - E(0)\ [D(t_1) - D(0)] \qquad (2.39)$$

where the subscript L has been introduced to identify $E_L(t_1)$ as the supposed lower bound to the exact value of $E(t_1)$.

Let $e_L(t_1)$ be defined so that

$$E_L(t_1) + e_L(t_1) = E(t_1) \qquad (2.40)$$

Now Equation (2.39) can be rewritten as follows

$$e_L(t_1)\ D(0) = -1 + E(0)\ [D(t_1) - D(0)] + E(t_1)\ D(0). \qquad (2.41)$$

Adding Equation (2.22) to Equation (2.40) yields

$$e_L(t_1)\ D(0) = E(0)\ [D(t_1) - D(0)] - \int_0^{t_1} E(t_1-\tau)\ \frac{d}{d\tau} D(\tau)\ d\tau. \qquad (2.42)$$

From Equation (2.16) one has

$$\int_0^{t_1} E(t_1-\tau)\ \frac{d}{d\tau} D(\tau)\ d\tau \leq E(0)\ [D(t_1) - D(0)]. \qquad (2.43)$$

Thus

$$e_L(t_1)\ D(0) \geq 0 \tag{2.44}$$

and, therefore,

$$e_L(t_1) \geq 0 \tag{2.45}$$

which means that $E_L(t_1)$ is the lower bound to $E(t_1)$.

At time $t_k = t_n$, Equation (2.5) can be written as

$$E_L(t_n)\ D(0) = 1 - \sum_{i=1}^{n} E_L(t_n - t_i)\ [D(t_i) - D(t_{i-1})]. \tag{2.46}$$

Let $e_L(t_n)$ be defined so that

$$E_L(t_n) + e_L(t_n) = E(t_n). \tag{2.47}$$

From Equations (2.46) and (2.47) it follows that

$$e_L(t_n)\ D(0) = -1 + E(t_n)\ D(0) + \sum_{i=1}^{n} E_L(t_n - t_i)\ [D(t_i) - D(t_{i-1})]. \tag{2.48}$$

Adding Equation (2.32) to Equation (2.48) yields

$$e_L(t_n)\ D(0) = \sum_{i=1}^{n} E_L(t_n - t_i)\ [D(t_i) - D(t_{i-1})] - \int_0^{t_n} E(t_n - \tau)\ \frac{d}{d\tau} D(\tau)\ d\tau. \tag{2.49}$$

Since D(t) is monotonically increasing, it follows that

$$\sum_{i=1}^{n} E_L(t_n-t_i)\,[D(t_i) - D(t_{i-1})] > 0 \qquad (2.50)$$

Also from Equation (2.16) one has

$$\int_0^{t_n} E(t_n-\tau)\,\frac{d}{d\tau}\,D(t)\,d\tau \leq \sum_{i=1}^{n} E(t_n-t_i)\,[D(t_i) - D(t_{i-1})]. \qquad (2.51)$$

Now Equation (2.49) can be transformed into the following inequality

$$e_L(t_n)\,D(0) \geq \sum_{i=1}^{n} E_L(t_n-t_i)\,[D(t_i) - D(t_{i-1})] - \sum_{i=1}^{n} E(t_n-t_i)\,[D(t_i) - D(t_{i-1})] \qquad (2.52)$$

which can be rewritten in the following form

$$e_L(t_n)\,D(0) \geq \sum_{i=1}^{n} [E_L(t_n-t_i) - E(t_n-t_i)][D(t_i) - D(t_{i-1})]. \qquad (2.53)$$

If $E_L(t)$ is smaller than E(t) in the above expression, the right hand side of the inequality will be the product of negative and positive values, and hence,

negative. Therefore here again the test fails, and nothing can be concluded about the conditions under which $e_L(t_n) \geq 0$.

Although no rigorous conclusions have been drawn about the validity of Equations (2.4) and (2.5), these equations provide a valid numerical approximation, as it is shown later in this chapter. Furthermore, the agreement of experimental and analytical results, shown in Chapter V, provides a strong verification of the good approximation obtained as an upper bound for the values of E(t) using Equation (2.4). Also it has been shown that for one interval of time, Equations (2.4) and (2.5) provide upper and lower bounds in the form

$$E_U(t_1) = \frac{1}{D(t_1)} \tag{2.54}$$

and

$$E_L(t_1) = \frac{1 - E(0)\,[D(t_1) - D(0)]}{D(0)} \tag{2.55}$$

2.4 Inversion of Discrete Experimental Data

The writer has tested both Equations (2.4) and (2.5), assuming for the values of D(t) those given by the expression proposed by Williams (19)

$$D(t) = D_g + \frac{D_e - D_g}{(1 + \frac{\tau_o}{t})^n}, \qquad (2.56)$$

where D_g is the compliance at short time, or glassy compliance, $D(0)$. D_e is the compliance at long time, or equilibrium compliance $D(\infty)$. And τ_o and n are parameters chosen to best fit the particular set of experimental data.

The numerical values adopted for D_g, D_e, τ_o, and n were found for the material studied in reference (13). With these values, the actual expression for the values of $D(t)$ was

$$D(t) + \left[2.0 + \frac{8.0}{(1 + \frac{13850000}{t})^{0.2}} \right] \times 10^{-6} \qquad (2.57)$$

The results obtained for (2.4) and (2.5) converged smoothly toward each other when the intervals of time were small (see Tables 2.1 and 2.2).* For time intervals of one hour or longer, the supposed lower bound solution showed some oscillations that would cross the upper bound for the first few steps, as can be seen in Tables 2.3 and 2.4.

A method for obtaining smooth solutions without oscillations for the lower bound will now be shown.

---

*The discrepancy shown in Tables 2.1 through 2.6 was calculated according to the formula:

$$\frac{\text{upper bound} - \text{lower bound}}{\text{lower bound}} \times 100.$$

In order to establish the time interval, two aspects of the problem must be taken into consideration. Use of large intervals results in undesirable oscillations of the lower bound. On the other hand, use of very small intervals would be impractical to span a reasonably long period of time.

The following procedure was adopted and used with satisfactory results on both counts. The method consisted essentially of redefining periodically the length of the intervals to be used. In this way, through the use of small intervals at the beginning of the inversion, oscillations were avoided. The use of larger and larger intervals as the experiment progressed made the method suitable to cover any practical period of time. There is no limit to the ways of redefining the time intervals to be used, and only practical considerations of the case involved will serve as a guide in this respect. Although a logarithmic increment of time is feasible, this would require some modifications in the computer program, which is written for equal intervals of time.

Tables 2.5 and 2.6 show the solutions obtained for two different redefinitions of the time intervals. In the case of Table 2.5, the inversion was stated with intervals equal to one second, and this was carried out

for a period of 180 seconds. Then the first redefinition was made in the following way:

E (60 seconds) becomes E (1 minute)
E (120 seconds) becomes E (2 minutes)
E (180 seconds) becomes E (3 minutes)

In this way, the values for one, two, and three minutes were obtained without any oscillations, and the inversion carried out again up to one hundred and eighty minutes. A similar redefinition was then made:

E (60 minutes) becomes E (1 hour)
E (120 minutes) becomes E (2 hours)
E (180 minutes) becomes E (3 hours).

After rerunning the inversion for thirty-six hours, a third redefinition took place:

E (12 hours) becomes E (1 half day)
E (24 hours) becomes E (2 half days)
E (36 hours) becomes E (3 half days).

The sequence of half-days was run for 360 steps, covering a period of time equal to six months.

Neither the upper nor the lower bound solutions showed any kind of oscillations. The greatest discrepancy between upper and lower bounds was of the order of 4% of the magnitude of the upper bound, and occurred in the fourth step of the inversion with intervals equal to half day. This figure dropped to 0.97% in the 13th step, and it was 0.06% at the end of the sixth-month period tested.

The redefinitions used in the solutions shown in Table 2.6 were similar to the ones just described, but the intervals were chosen so as to be compatible with those that can be obtained in the laboratory, using simple equipment: a dial gauge and a timer. This means that the closest that the readings can be spaced would be from .06 to .10 minutes apart, when the help of a second operator is used.

In this second example, the first 30 steps of the inversion were run with intervals equal to six seconds. The following redefinition was used

E (10th interval) becomes E (1 minute)
E (20th interval) becomes E (2 minutes)
E (30th interval) becomes E (3 minutes).

This was the only redefinition used, and the inversion was then carried out for 768 minutes.

Although the last example took the values of D(t) to be inverted from Equation (2.57), it is obvious that those same values could have been taken from a set of discrete values obtained from lab observations. The only condition imposed upon the set of D(t) values is that an entry should exist for every time interval considered in the inversion. This condition does not present any practical difficulty, since the time intervals considered in the inversion not only are compatible with those readily obtainable in the laboratory, but also happened to provide a set of points well-spaced to plot a time-deflection curve

during the course of the laboratory test, as will be shown in Chapter IV.

Finally, Table 2.7 shows the results of an inversion when actual discrete laboratory data are used for the creep compliance values. The time interval redefinition used in the frame analysis, explained in Section 3.5 and Figure 3.6, was the one used in this example. Furthermore, the values of E(t) shown in Table 2.7, which are the upper bounds given by Equation (2.4) were the ones adopted as true values of E(t) in the theoretical analysis of framed structures of Chapter III.

TABLE 2.1.--Upper and lower bounds for E(t). Time intervals equal to one second. Total period covered equal to three minutes.

Time (seconds)	Upper Bound (psi)	Lower Bound (psi)	Discrepancy (%)
0	500000	500000	.00
1	469140	467110	.43
2	464830	464380	.10
3	462060	461690	.08
4	459980	459680	.07
5	458290	458030	.06
6	456860	456630	.05
7	455620	455420	.04
8	454520	454330	.04
9	453530	453360	.04
10	452620	452460	.04
15	449000	448880	.03
20	446290	446190	.02
40	439220	439150	.01
60	434720	434670	.01
80	431360	431320	.01
100	428660	428620	.01
120	426380	426350	.01
140	424410	424380	.01
160	422660	422640	.01
180	421100	421080	.01

TABLE 2.2.--Upper and lower bounds for E(t). Time intervals equal to one minute. Total period covered equal to three hours.

Time (minutes)	Upper Bound (psi)	Lower Bound (psi)	Discrepancy (%)
0	500000	500000	.00
1	435090	425400	2.28
2	426690	425440	.29
3	421370	419850	.36
4	417410	416260	.28
5	414230	413250	.24
6	411560	410700	.21
7	409260	408490	.19
8	407230	406530	.17
9	405410	404760	.16
10	403750	403160	.15
15	397200	396750	.11
20	392350	391990	.09
40	380010	379790	.06
60	372350	372190	.04
80	366740	366610	.04
100	362270	362160	.03
120	358550	358460	.03
140	355360	355280	.02
160	352570	352490	.02
180	358070	350000	.02

TABLE 2.3.--Upper and lower bounds for E(t). Time intervals equal to one hour. Total period covered equal to 30 days.

Time (hours)	Upper Bound (psi)	Lower Bound (psi)	Discrepancy (%)
0	500000	500000	.00
1	373590	330810	12.93
2	359540	362900	-.93
3	350910	344140	1.97
4	344610	341950	.78
5	339630	336620	.90
6	335510	333120	.72
7	331980	329810	.66
8	328900	326970	.59
9	326170	324410	.54
10	323700	322090	.50
11	321460	319970	.47
12	319410	318010	.44
13	317510	316200	.41
14	315750	314510	.39
16	312550	311450	.35
18	309710	308710	.32
20	307170	306250	.30
24	302730	301940	.26
28	298950	298260	.23
32	295660	295040	.21
36	292750	292190	.19

TABLE 2.4.--Upper and lower bounds for E(t). Time intervals equal to twelve hours. Total period covered equal to six months.

Time (half days)	Upper Bound (psi)	Lower Bound (psi)	Discrepancy (%)
0	500000	500000	.00
1	321300	221900	44.79
2	304220	335230	-9.25
3	293990	268210	9.61
4	286650	290610	-1.36
5	280930	272250	3.19
6	276250	274640	.58
7	272280	268040	1.58
8	268840	266430	.90
9	265800	262960	1.08
10	364080	260810	.87
15	252630	250960	.66
20	245230	243940	.53
30	234840	233950	.38
40	227530	226850	.30
60	217320	216850	.22
120	200200	199960	.12
180	190460	190300	.09
240	183690	183570	.07
300	178530	178430	.06
360	174380	174300	.05

TABLE 2.5.--Upper and lower bounds for E(t). Time interval redefined as the inversion proceeds. Intervals used: 1 second, 1 minute, 1 hour, 12 hours. Total period covered equal to six months.

Time (hours)	Upper Bound (psi)	Lower Bound (psi)	Discrepancy (%)
1	372360	372190	.05
2	358550	358450	.03
3	350070	350000	.02
4	344680	338830	1.73
5	339680	336490	.95
6	335550	332400	.95
7	332020	239390	.80
8	328930	326560	.73
36	292760	292110	.22
(half days)			
1	319430	317760	.42
2	302740	391820	.31
3	292760	292110	.22
4	286820	274910	4.33
5	281050	276870	1.51
6	276330	270240	2.26
7	272350	268360	1.49
8	268900	264770	1.56
50	221900	221200	.31
100	204660	204300	.17
220	185730	185560	.09
360	174390	174290	.06

TABLE 2.6.--Upper and lower bounds for E(t). Time interval redefined as the inversion proceeds. Intervals used: 6 seconds, 1 minute. Total period covered equal to 768 minutes.

Time (minutes)	Upper Bounds (psi)	Lower Bounds (psi)	Discrepancy (%)
1	434781	434489	.07
2	426422	426241	.04
3	421134	420998	.03
4	417418	415936	.36
5	414238	413156	.26
6	411569	410616	.23
8	407231	406468	.19
10	403757	403112	.16
12	400847	400285	.14
16	396124	395670	.11
20	392350	391965	.10
24	389194	388858	.09
32	384083	383812	.07
40	380007	379778	.06
48	376605	376405	.05
64	371108	370947	.04
96	363094	362976	.03
160	352566	352486	.02
256	342473	342418	.02
384	333471	333431	.01
768	317509	317486	.01

TABLE 2.7.--Upper bound of E(t) obtained from discrete values of D(t). Time interval redefined as explained in Section 3.5. Total period covered, 768 minutes.

Time (minutes)	D(t) (sq. in./lb.)	E(t) (lbs./sq. in.)
1	2.275×10^{-6}	4.394×10^{5}
2	2.312×10^{-6}	4.323×10^{5}
3	2.337×10^{-6}	4.276×10^{5}
4	2.356×10^{-6}	4.242×10^{5}
5	2.372×10^{-6}	4.213×10^{5}
6	2.386×10^{-6}	4.187×10^{5}
8	2.408×10^{-6}	4.149×10^{5}
10	2.427×10^{-6}	4.116×10^{5}
12	2.444×10^{-6}	4.087×10^{5}
16	2.472×10^{-6}	4.040×10^{5}
20	2.495×10^{-6}	4.002×10^{5}
24	2.516×10^{-6}	3.968×10^{5}
32	2.550×10^{-6}	3.915×10^{5}
40	2.581×10^{-6}	3.866×10^{5}
48	2.612×10^{-6}	3.817×10^{5}
64	2.662×10^{-6}	3.745×10^{5}
96	2.739×10^{-6}	3.634×10^{5}
160	2.847×10^{-6}	3.494×10^{5}
256	2.954×10^{-6}	3.368×10^{5}
384	3.048×10^{-6}	3.260×10^{5}
768	3.208×10^{-6}	3.099×10^{5}

CHAPTER III

FRAME ANALYSIS

3.1 Elastic Analysis

The governing equation for elastic beam-columns is (17)

$$EI \frac{d^4}{dx^4} y(x) + N\frac{d^2}{dx^2} y(x) = q(x) \qquad (3.1)$$

where EI represents the flexural rigidity of the beam in the plane of bending, N is the axial load, and q is the load distributed along the member length.

In the theory of matrix structural analysis, the expression

$$\{X\} = [K]^{-1} \{P\} \qquad (3.2)$$

is well known, where the column matrix {X} represents the structure joint displacement vector, [K] is the structure stiffness matrix, and {P} is the load vector. Brackets {} will be used throughout this work to indicate a column matrix.

The elements of the load vector {P} act only at the joints of the structure. In general, however, a structure will also have loads acting on the members. When this is the case, in order to use Equation (3.2), the loads

acting on the members must be transformed to equivalent joint loads. Then the vector {P} may be considered as made up of two parts

$$\{P\} = \{W\} + \{Q\} \tag{3.3}$$

where {W} represents the actual loads acting at the joints, and {Q} is the equivalent joint loads. {P} is then called the combined joint load vector.

The vector {Q} is evaluated in such a manner that the resulting joint displacements of the structure calculated from Equation (3.2), when using the combined joint load vector {P}, are the same as the displacements produced by the actual loads. Furthermore, the support reactions for the structure subjected to the combined loads are the same as the support reactions caused by the actual loads. The evaluation of {Q} and its properties can be found in any standard matrix structural analysis textbook, for example, reference (8).

Unfortunately the substitution of loads acting on the members by the equivalent joint load vector {Q} will not preserve the actual transversal deflections, y(x), along those members which originally were loaded. When the actual force acting on the member is replaced by the equivalent joint load, and included in the combined joint load vector {P}, although the end displacements remain unchanged, the transversal displacements along the member

are no longer equal to y(x). We call these displacements, caused by the combined joint load vector {P}, u(x). To find the actual deflections y(x), a correction v(x) has to be added to u(x). The deflections v(x) are obtained by loading the member with its original load system, while keeping the ends clamped (10). It can then be written

$$y(x) = u(x) + v(x). \tag{3.4}$$

3.2 Viscoelastic Analysis

For viscoelastic beam-columns LaPalm (13) shows that Equation (3.1) takes the form

$$IE(t)\,\frac{\partial^4}{\partial x^4}\,y(x,0) + \int_0^t IE(t-\tau)\,\frac{\partial}{\partial \tau}\,[\frac{\partial^4}{\partial x^4}\,y(x,\tau)]\,\partial\tau + N(t)\,\frac{\partial^2}{\partial x^2}\,y(x,t) = q(x,t) \tag{3.5}$$

with an upper bound given by the solution of

$$IE(t_k-t_{k-1})\,\frac{\partial^4}{\partial x^4}\,y(x,t_k) + N(t_k)\,\frac{\partial^2}{\partial x^2}\,y(x,t_k) = q(x,t_k) - I\sum_{i=1}^{k-1}\,[E(t_k-t_{i-1}) - E(t_k-t_i)]\,\frac{\partial^4}{\partial x^4}\,y(x,t_i) \tag{3.6}$$

and a lower bound given by the solution of

$$IE(t_k-t_{k-1}) \frac{\partial^4}{\partial x^4} y(x,t_k) + N(t_k) \frac{\partial^2}{\partial x^2} y(x,t_k)$$

$$= q(x,t_k) - I \sum_{i=0}^{k-1} [E(t_k-t_i) - E(t_k-t_{i+1})] \frac{\partial^4}{\partial x^4} (x,t_i) \tag{3.7}$$

subject to boundary conditions given in terms of transversal displacements and rotations at the ends of the member, as shown in section 3.3.

The left-hand sides of both Equation (3.6) and (3.7) have the same form as Equation (3.1), while the right-hand sides, representing the forcing function, are made up of the actual load $q(x,t_k)$ at time t_k, plus a fictitious load derived from the history of the solution.

Now the writer proposes to parallel the relation between Equation (3.1) and (3.2), with that between Equation (3.6) or (3.7) and

$$\{X(t)\} = [K(t)]^{-1} \{P(t)\} \tag{3.8}$$

Equation (3.8) produces the joint displacement history of framed structures made of linear viscoelastic materials, as the writer intends to show. At a given time, t_k, Equation (3.8) becomes

$$\{X(t_k)\} = [K(t_k)]^{-1}\{P(t_k)\} \tag{3.9}$$

which could be identified with Equation (3.2), except for the vector $\{P(t_k)\}$ that has a peculiarity of its own.

The vector $\{P\}$ in Equation (3.2) has two parts, given by Equation (3.3), where $\{Q\}$ represents the equivalent joint load, taking the place of the actual distributed loading, $q(x)$, as appears in the governing Equation (3.1). Likewise, it follows that the vector $\{P(t_k)\}$ in Equation (3.9) is given by

$$\{P(t_k)\} = \{W(t_k)\} + \{Q(t_k)\} + \{F(t_k)\} \tag{3.10}$$

where the new term $\{F(t_k)\}$ is a fictitious equivalent joint load vector taking the place of the forcing term

$$I \sum_{i=1}^{k-1} [E(t_k - t_{i-1}) - E(t_k - t_i)] \frac{\partial^4}{\partial x^4} y(x,t_i)$$

of the governing Equation (3.6), or

$$I \sum_{i=0}^{k-1} [E(t_k - t_i) - E(t_k - t_{i+1})] \frac{\partial^4}{\partial x^4} y(x,t_i)$$

of the governing Equation (3.7). This means that the vector $\{F\}$ is a function of all previous deformed configurations of the structure. This could be rephrased, saying that the deflections to be obtained at a given

time, t_k, will depend not only on the actual loading at that moment, but also on the whole previous deflection history.

Before an evaluation of $\{F(t_k)\}$ can be attempted, the set of previous solutions $y(x,t_1)$, $y(x,t_2)$, ... , $y(x,t_{k-1})$ must be available.

3.3 Transversal Deflections

At a given time, t_k, $y(x,t_k)$ can be written as $y_k(x)$, and considered as a function of x alone. The Equation (3.6) may be written as

$$IE(t_k-t_{i-1}) \frac{d^4}{dx^4} y_k(x) + N_k \frac{d^2}{dx^2} y_k(x)$$

$$= q_k(x) - I\sum_{i=1}^{k-1} [E(t_k-t_{i-1}) - E(t_k-t_i)] \frac{d^4}{dx^4} y_i(x) \qquad (3.11)$$

The handling of the distributed load q(x) is a well-established procedure in the analysis of elastic structures. The reader is referred to reference (8). Therefore, since its consideration at this point would only make the study more cumbersome, without producing new results, we will drop it now, and consider loading applied at structure joints alone. Equation (3.11) becomes, finally

$$y_k^{IV} + k_k^2 y_k^{II} = f_k \qquad (3.12)$$

where

$$y_k^{IV} = \frac{d^4}{dx^4} y_k(x)$$

$$y_k^{II} = \frac{d^2}{dx^2} y_k(x)$$

$$k_k^2 = \frac{N_k}{IE(t_k - t_{i-1})}$$

$$f_k = \frac{\sum_{i=1}^{k-1} [E(t_k - t_{i-1}) - E(t_k - t_i)] \frac{d^4}{dx^4} y_k(x)}{E(t_k - t_{i-1})}$$

The solution of Equation (3.12) is subject to the boundary conditions

$$\{Y\} = \{Y^*\} \tag{3.13}$$

where

$$\{Y\} = \begin{Bmatrix} y \Big|_{x=o} \\ \frac{dy}{dx} \Big|_{x=o} \\ y \Big|_{x=L} \\ \frac{dy}{dx} \Big|_{x=L} \end{Bmatrix} \equiv \begin{Bmatrix} y(O) \\ y'(O) \\ y(L) \\ y'(L) \end{Bmatrix} \tag{3.14}$$

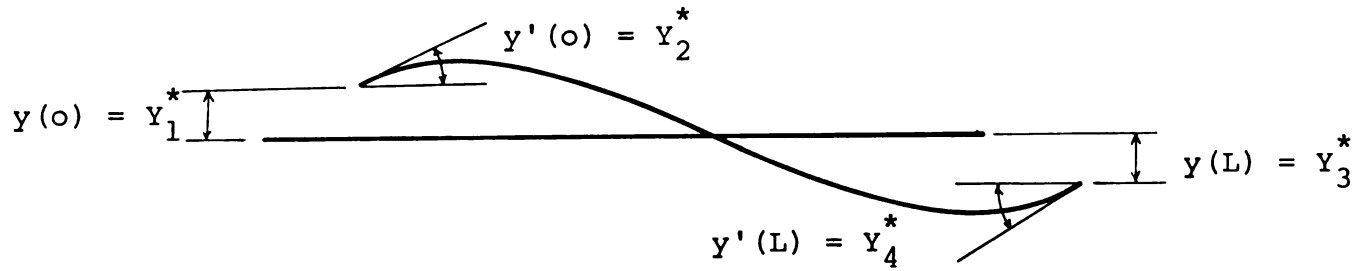

Figure 3.1.--Member boundary values.

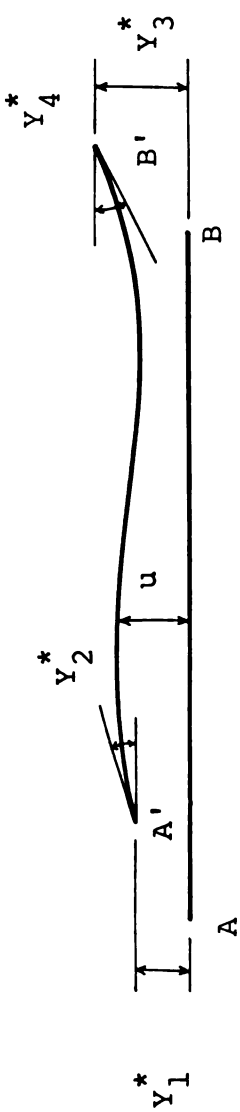

Figure 3.2.--Deflections u and boundary values.

and {Y*} represents the member end displacements obtained from the structure joint displacements, {X}, in Equation (3.9), see Figure 3.1.

The value of f_k in Equation (3.12) is a function of the solutions $y_1(x)$, $y_2(x)$, ... , $y_{k-1}(x)$, obtained at times t_1, t_2, ... , t_{k-1}. Therefore, at time t_1, $f_1 = 0$, and the initial solution $y_1(x)$ is obtained from the homogeneous case of Equation (3.12). Instead of solving equation (3.12) directly, the value of y(x) will be obtained in a manner similar to the procedure followed for the elastic case with equation (3.4).

Let $u_k(x)$ be the transversal displacements obtained for a member at a given time t_k, when the actual loading acting on this rember has been substituted by equivalent joint loads and incorporated in the combined joint load vector $\{P(t_k)\}$ in Equation (3.9). The displacements $u_k(x)$ are not equal to the displacements $y_k(x)$ obtained from the actual load system. A correction $v_k(x)$, defined later in this section, will be needed. Let $u \equiv u_k(x)$. Then the deflections u, shown in Figure 3.2, are given by the equation

$$u^{IV} + k^2 u^{II} = 0 \qquad (3.15)$$

under the boundary conditions

$$\{U\} = \{Y^*\} \tag{3.16a}$$

where {U} is defined in a manner similar to the way {Y} was defined for boundary condition (3.13), i.e., by the column matrix

$$\{U\} = \{u(o) \quad u'(o) \quad u(L) \quad u'(L)\} \tag{3.16b}$$

and {Y*} is obtained from the structure joint deflections.

In order to obtain the member deflections y for the actual loads, a correction, v, must be added to the deflections, u. In order to obtain this correction, we clamp the ends A' and B', in Figure 3.2 and apply the distributed load, f, as shown in Figure 3.3.

The deflections, v, are given by the equation

$$v^{IV} + k^2 v^{II} = f \tag{3.17}$$

subjected to the homogeneous boundary conditions

$$\{V\} = \{O\} \tag{3.18}$$

where, as before,

$$\{V\} = \{v(o) \quad v'(o) \quad v(L) \quad v'(L)\} \tag{3.19}$$

and {Y*} is obtained from the structure joint displacements.

Finally, because of linearity of the governing equation, the member deflections due to the actual loads are given by

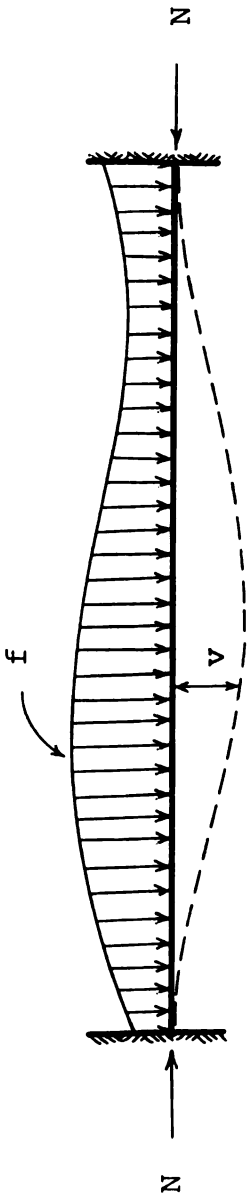

Figure 3.3.--Deflections v.

$$y = u + v \tag{3.20}$$

Likewise, the fourth derivations of the deflections will be given by

$$y^{IV} = u^{IV} + v^{IV} \tag{3.21}$$

3.3.1 Deflection Due to Combined Joint Loads

Three different cases will be considered for Equation (3.15), corresponding to a member under tension, compression or no axial load.

For no axial load, the deflections u will be given by equation

$$u^{IV} = 0 \tag{3.22}$$

with boundary conditions

$$\{U\} = \{Y^*\} \tag{3.23}$$

yielding the solution

$$u = A_1x^3 + A_2x^2 + A_3x + A_4 \tag{3.24}$$

where

$$A_1 = \frac{2}{L^3} Y_1^* + \frac{1}{L^2} Y_2^* - \frac{2}{L^3} Y_3^* + \frac{1}{L^2} Y_4^*$$

$$A_2 = -\frac{3}{L^2} Y_1^* - \frac{2}{L} Y_2^* + \frac{3}{L^2} Y_3^* - \frac{1}{L} Y_4^*$$

$$A_3 = Y_2^*$$

$$A_4 = Y_1^* \qquad (3.25)$$

and the fourth derivative is obviously given by Equation (3.22).

For members under compression, the governing equation will be

$$u^{IV} + k^2 u^{II} = 0 \qquad (3.26)$$

with boundary conditions (3.23), yielding the solution

$$u = B_1 \cos kx + B_2 \sin kx + B_3 x + B_4 \qquad (3.27)$$

with the fourth derivative given by

$$u^{IV} = B_1 k^4 \cos kx + B_2 k^4 \sin kx \qquad (3.28)$$

where

$$B_1 = \frac{(-Y_1^*-LY_2^*+Y_3^*)(k\cos kL-k) - (-Y_2^*+Y_4^*)(\sin kL-kL)}{(\cos kL-1)(k\cos kL-k) - (-k\sin kL)(\sin kL-kL)}$$

$$B_2 = \frac{(\cos kL-1)(-Y_2^*+Y_4^*) - (-k\sin kL)(-Y_1^*-LY_2^*+Y_3^*)}{(\cos kL-1)(k\cos kL-k) - (-k\sin kL)(\sin kL-kL)}$$

$$B_3 = Y_2^* - A_2k$$

$$B_4 = Y_1^* - A_1 \qquad (3.29)$$

Finally, for members under tension the governing equation becomes

$$u^{IV} - k^2u^{II} = 0 \qquad (3.30)$$

with boundary conditions (3.23), yielding the solution

$$u = C_1\cosh kx + C_2\sinh kx + C_3x + C_4 \qquad (3.31)$$

with the fourth derivative given by

$$u^{IV} = C_1k^4\cosh kx + C_2k^4\sinh kx \qquad (3.32)$$

where

$$C_1 = \frac{(-Y_1^*-Y_2^*L+Y_3^*)(k\cosh kL-k) - (-Y_2^*+Y_4^*)(\sinh kL-kL)}{(\cosh kL-1)(k\cosh kL-k) - (k\sinh kL)(\sinh kL-kL)}$$

$$C_2 = \frac{(\cosh kL-1)(-Y_2^*+Y_4^*) - (k\sinh kL)(-Y_1^*-Y_2^*L+Y_3^*)}{(\cosh kL-1)(k\cosh kL-k) - (k\sinh kL)(\sinh kL-kL)}$$

$$C_3 = Y_2^* - C_2 k$$

$$C_4 = Y_1^* - C_1 \qquad (3.33)$$

3.3.2 Deflection Corrections Due to Distributed Loads

The value of k in Equation (3.17) changes with time, and so will the form of the solution, which would become complex and awkward to handle in a general algebraic formulation. More desirable and practical, when digital computers are to be used, would be a numerical solution.

A finite difference method will be used to approximate the second and fourth derivatives, with an error of the order of h^2, as follows, see reference (16):

$$v_i^{II} = \frac{v_{i-1} - 2v_i + v_{i+1}}{h^2} \qquad (3.34)$$

$$v_i^{IV} = \frac{v_{i-2} - 4v_{i-1} + 6v_i - 4v_{i+1} + v_{i+2}}{h^4} \qquad (3.35)$$

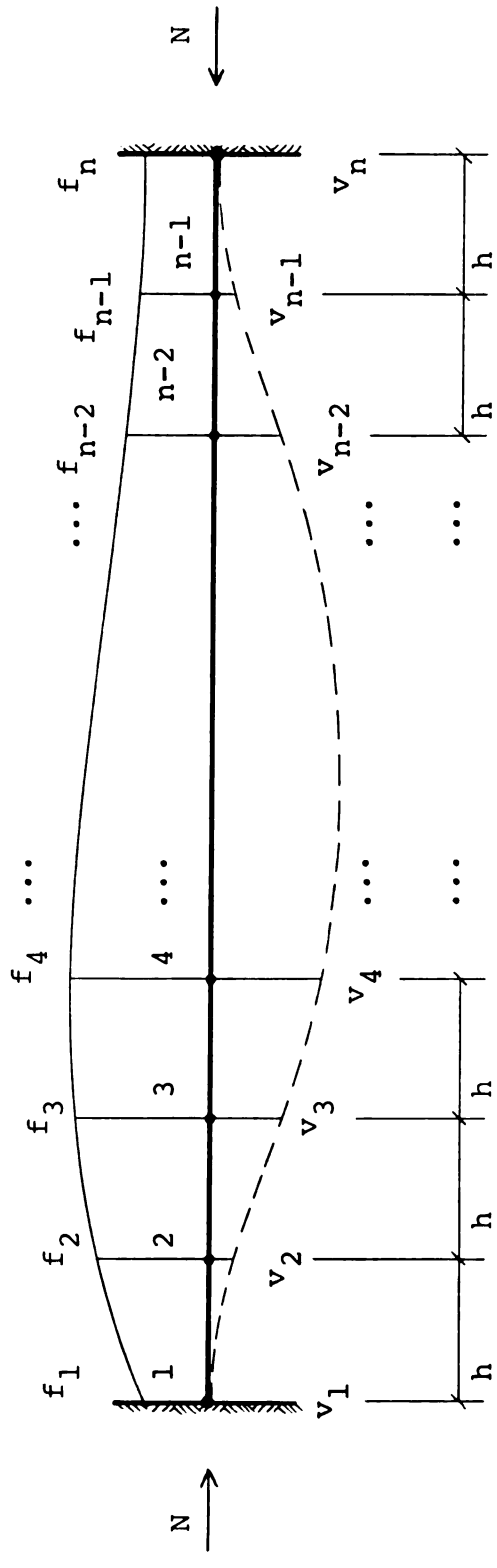

Figure 3.4.--Member divided into n-1 equal parts.

Dividing the member under analysis in n-1 equal parts with n nodes (see Figure 3.4), by substitution of relations (3.34) and (3.35) into Equation (3.17), we can write

$$v_{i-2} + (h^2k^2-4)v_{i-1} + (-2h^2k^2+6)v_i + (h^2k^2-4)v_{i+1} + v_{i+2} = h^4f_i \qquad (3.37)$$

From Equation (3.37) and boundary conditions (3.18), the following system of equations is obtained:

$$v_1 = 0$$

$$(-2h^2k^2+7)v_2 + (h^2k^2-4)v_3 + v_4 = h^4f_2$$

$$(h^2k^2-4)v_2 + (-2h^2k^2+6)v_3 + (h^2k^2-4)v_4 + v_5 = h^4f_3$$

$$v_2 + (h^2k^2-4)v_3 + (-2h^2k^2+6)v_4 + (h^2k^2-4)v_5 + v_6 = h^4f_4$$

$$v_3 + (h^2k^2-4)v_4 + (-2h^2k^2+6)v_5 + (h^2k^2-4)v_6 + v_7 = h^4f_5$$

$$\cdot \quad \cdot \quad \cdot \quad \cdot \quad \cdot \quad \cdot \quad \cdot$$

$$\cdot \quad \cdot \quad \cdot \quad \cdot \quad \cdot \quad \cdot \quad \cdot$$

$$v_{n-5} + (h^2k^2-4)v_{n-4} + (-2h^2k^2+6)v_{n-3} + (h^2k^2-4)v_{n-2} + v_{n-1} = h^4f_{n-3}$$

$$v_{n-4} + (h^2k^2-4)v_{n-3} + (-2h^2k^2+6)v_{n-2} + (h^2k^2-4)v_{n-1}$$

$$= h^4 f_{n-2}$$

$$v_{n-3} + (h^2k^2-4)v_{n-2} + (-2h^2k^2+7)v_{n-1} = h^4 f_{n-1}$$

$$v_n = 0 \qquad (3.38)$$

This system of linear algebraic simultaneous equations is readily solved for v. In the present case, the Gauss elimination method (6) was used. The listing of the computer program appears in Appendix B.

Knowing the values of v, the fourth derivative, v^{IV}, is obtained by numerical differentiation. The derivatives corresponding to the nodes 1 and n were obtained by forward and backward differences, respectively, using the following expressions (16), with an error of the order of h^2:

$$v_i^{IV} = \frac{3v_i - 14v_{i+1} + 26v_{i+2} - 24v_{i+3} + 11v_{i+4} - 2v_{i+5}}{h^4} \qquad (3.39)$$

$$v_i^{IV} = \frac{-2v_{i-5} + 11v_{i-4} - 24v_{i-3} + 26v_{i-2} - 14v_{i-1} + 3v_i}{h^4} \qquad (3.40)$$

while for the nodes 2, 3, ... , n-1, Equation (3.35) was used.

Applying Equations (3.20) and (3.21), one is now in a position to evaluate the deflections and their fourth derivatives for each member of the structure. The deflections y obtained at times t_k, k = 1, 2, ... , will give the deformation history of the structure, while the fourth derivatives, y^{IV}, at times t_1, t_2, ... t_k, will provide the forcing function, f, for time t_{k+1}, according to Equation (3.12).

3.4 Equivalent Joint Loads

As it was pointed out earlier in this chapter, the forcing function, f, in Equation (3.12) acts as a distributed load, and in order to take into consideration its effect on the structural analysis, an equivalent joint load, F, must be formed, to be added to the structural loading, as shown in Equation (3.10).

The evaluation of F will parallel that of Q, with f playing the role of q. The distributed load q can, in many practical cases, be approximated by a simple function of x, for which the reactions are often found tabulated, or easily calculated. In the case of f, all one has is a set of discrete values, as many as thought necessary, and a general algebraic solution is not readily available. Therefore a numerical procedure will be used.

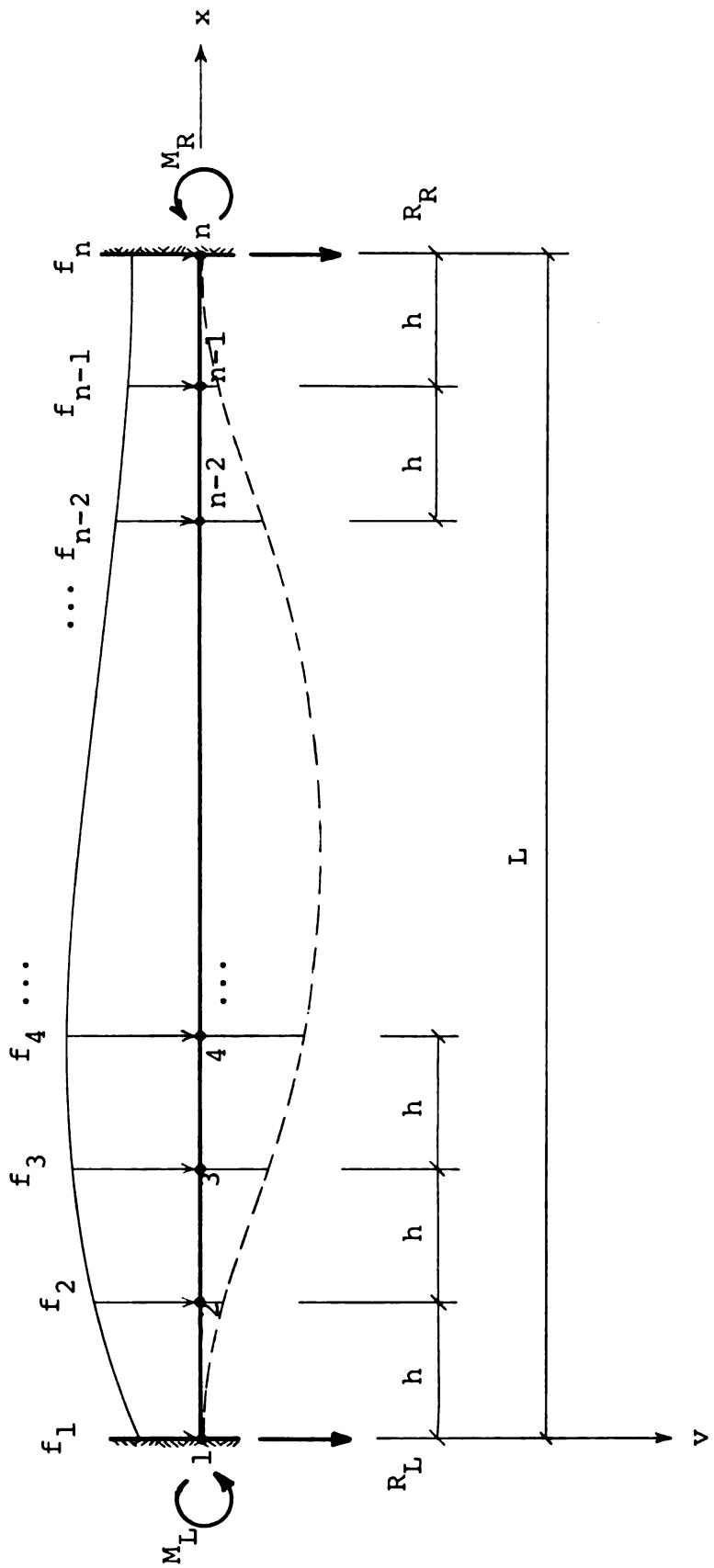

Figure 3.5.--Fixed end member with loading and end reactions shown in the positive direction.

Loading the member with the function f, as shown in Figure 3.4, Equation (3.37) will give the values of the deflections v. Then, neglecting the effects of shearing deformations and shortening of the beam axis, one has, for an elastic material (17)

$$EI \frac{d^2y}{dx^2} = -M \tag{3.41}$$

Applying the correspondence principle (5), Equation (3.41) becomes, for a linear viscoelastic material, at time t_k,

$$M_k = - E(t_k) \; I \; y_k^{II} \tag{3.42}$$

From Equation (3.42), one has

$$M_L = - E(t_k) \; I \; y^{II}(0) \tag{3.43}$$

$$M_R = - E(t_k) \; I \; y^{II}(L) \tag{3.44}$$

where M_L and M_R represent the end moment reactions for $x = 0$ and $x = L$, respectively. The subscripts L and R stand for left and right, not to be confused with L which represents the length of the member (see Figure 3.5).

Taking moments about point n and 1, one obtains

$$R_L = \frac{M_L - M_R}{L} - \frac{1}{L} \sum_{i=1}^{n-1} \frac{1}{2}(f_i + f_{i+1})h[L - \frac{h}{2} - (i-1)h] \tag{3.45}$$

$$R_R = \frac{M_R - M_L}{L} - \frac{1}{L} \sum_{i=1}^{n-1} \frac{1}{2}(f_i + f_{i+1})h[\frac{h}{2} + (i-1)h] \qquad (3.46)$$

where h represents the length of the n-1 equal segments, in which each member of the structure is divided.

The negative of the values obtained for M_L, M_R, R_L and R_R for each member of the structure, are applied as loads at the structure joints, and the set of these loads forms the vector F.

3.5 Numerical Computer Solution

The numerical solution of Equation (3.12) by means of digital computers faces the problem of storage, since the forcing function at a given time, t_k, will be a function of all previous deformed configurations. If the structure has m members, each divided in n-1 parts, and the period of time to be analyzed has k time units, the required storage space would be m(n-1) k. In this way, the length of the period of time for which the structure can be analyzed is limited considerably, even if auxiliary storage space, such as tapes, drums, etc., is used.

In order to avoid this difficulty, a redefinition of the time interval is used in this work. Figure 3.6 represents schematically this redefinition. The t-axis serves as basic time reference, and it will give the structure's age in minutes. The r-axis represents the

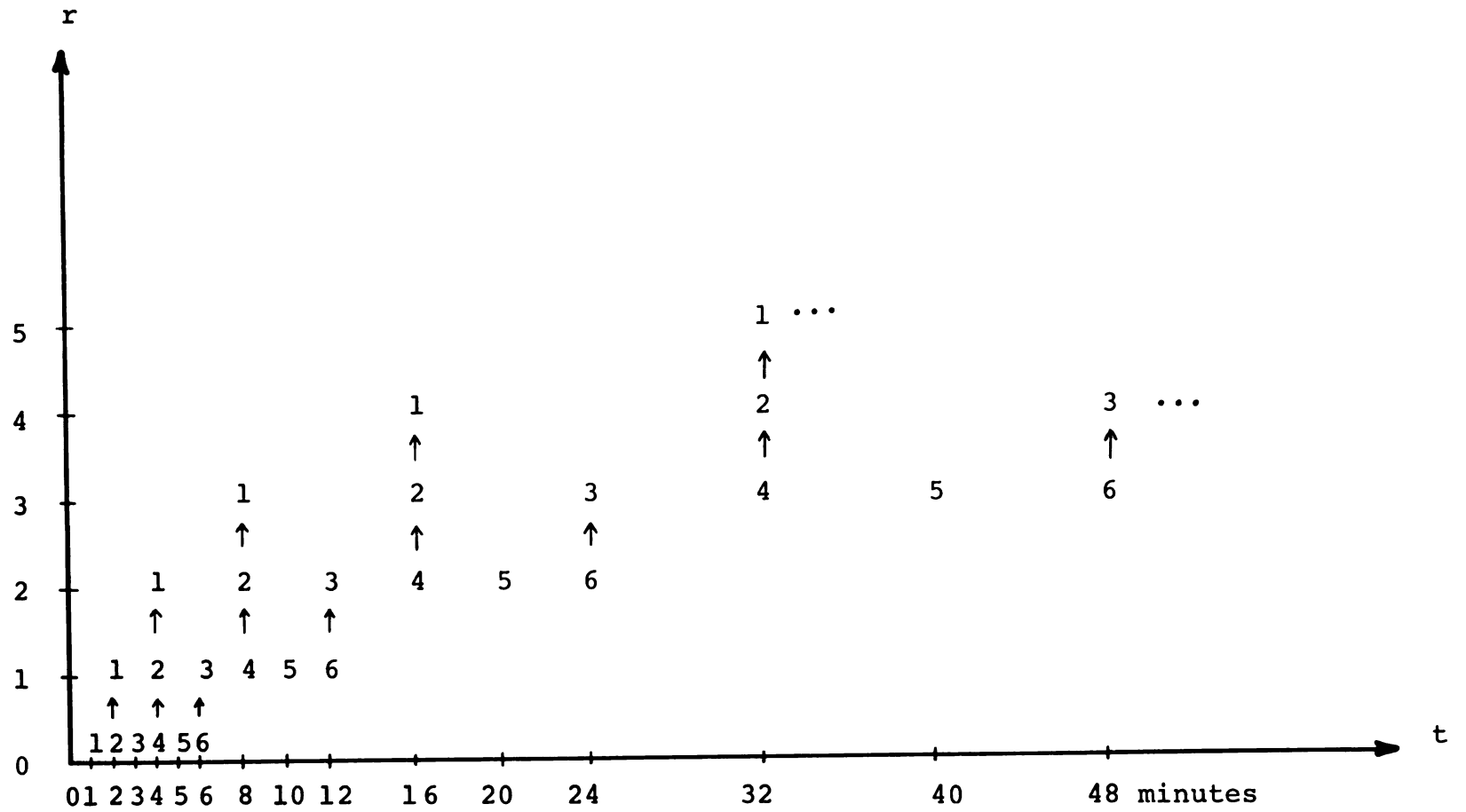

Figure 3.6.--Time interval redefinition.

cycle or iteration, i.e., it tells how many times the time intervals have been redefined. The numbers on the tr-plane are the time interval labels, which will be represented by the letter i.

Every cycle goes from 1 to 6, and is defined in such a manner that the age of the structure during iteration r at interval i will be given by

$$t = i \cdot 2^{r} \text{ minutes} \tag{3.47}$$

In this way, the storage required of past deformed configurations to produce the forcing function f, will reduce to $6m(n-1)$. The choice of 6 intervals in each cycle was arbitrary to a great extent, and a different number might be shown to produce better results. Six was chosen because it is a small number, offers three points to overlap with the past known data, and advances an equal amount toward new data.

At this point, one has all the necessary means to produce a numerical solution by programming a high-speed digital computer. A concise general flow chart of such a program appears on Chart 3.1. Double-lined boxes indicate that the step is obtained by means of a sub-routine subprogram.

The Chart 3.1 starts with the label DATA, under which are included the general information about the structure properties, loads, member subdivision, time

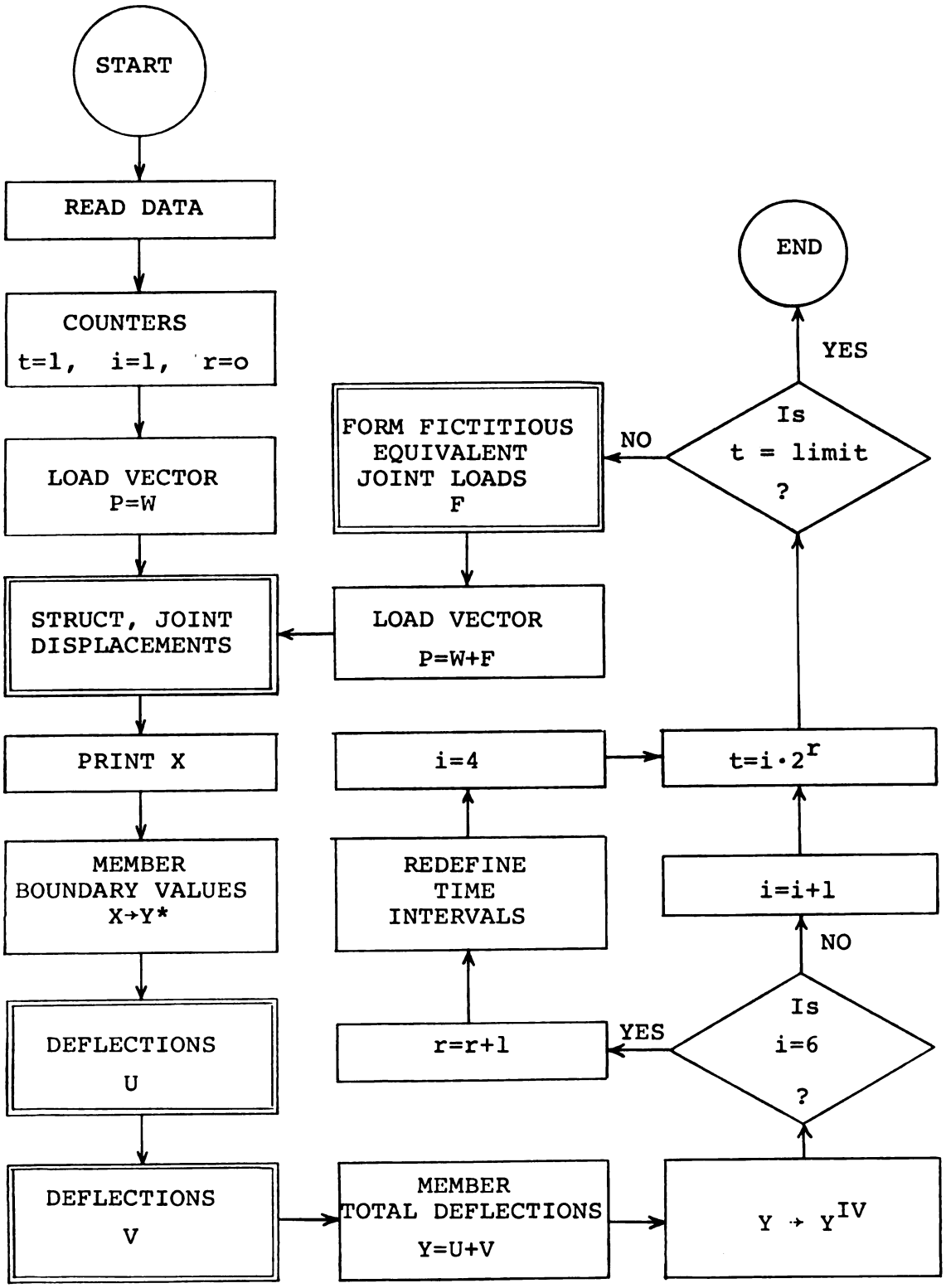

Chart 3.1.--Concise general flow chart.

limit, etc. If the relaxation modulus, E(t), is not given as an algebraic function, its tabulated set of values will be also read at this moment.

To define time, three counters will be used. Basic time, in minutes is represented by t, the time interval by i, and the cycle number, or iteration, by r. So the program starts by setting t=1, i=1, and r=0.

The actual loads applied at the joints are given by the vector W. So, at time t=1, since the structure was previously undeformed, the load vector P will equal W.

Now keeping the time fixed, an elastic analysis is run, by means of a subroutine. The analysis follows the procedure outlined by Wang (18) in a second order structural analysis, taking into consideration the effect of axial forces on the flexural stiffness of the members, and enforcing equilibrium in accordance with the deformed geometry of the structure. The listing of this subroutine is not given in Appendix B, and the reader is referred to reference (18).

The deflections u and v were defined previously, and are calculated by two separate subroutines, whose listing appears in Appendix B.

Finally, the fictitious equivalent joint loads are obtained by the finite difference method described in paragraph 3.4, and the program listing can also be found in Appendix B.

3.6 Quasi-Elastic Solution

If the effect of axial force on the flexural stiffness of the structure is neglected, the solution can be obtained by application of the super-position principle (7), i.e.,

$$X(t) = S(t)\ P(O) + \int_{o}^{t} S(t-\tau)\ \frac{d}{d\tau}\ P(\tau)\ d\tau \qquad (3.48)$$

where S(t) is the time-dependent solution for a unit step loading, and P(t) is the time-dependent load.

If the structure is subjected to a constant load, P = P(O), as in the case being considered, the integral of equation (3.48) will vanish, and for any given time t_k, one obtains

$$X(t_k) = S(t_k)\ P \qquad (3.49)$$

The difference between Equation (3.40) and Equation (3.2), is that while for the elastic case the flexibility matrix is kept fixed, for the quasi-elastic case at every time, t_k, the modulus of elasticity, E, is replaced by the corresponding value of the relaxation modulus. Of course, as it has been pointed out above, the flexibility matrix $S(t_k)$, unlike $K^{-1}(t_k)$ in Equation (3.9), does not include the effect of the axial force in the members' stiffness. The solution of Equation (3.49) provides an

alternative approximation to the viscoelastic deflection history of the structure, called the quasi-elastic solution.

CHAPTER IV

LABORATORY WORK

4.1 Materials

The materials, equipment, and laboratory tests are similar to those used by LaPalm (13). At risk of being repetitious, a brief description of the laboratory work will be given in this chapter.

The material used was epoxy resin ARALDITE 502 in combination with ARALDITE Hardener 951, both manufactured by CIBA Products Company, Summit, New Jersey. This mixture cures in a short time at room temperature, has a wide linear range, and can be reproduced. Also, individual pieces can be welded together, making possible models of different shapes. These properties are claimed by the manufacturer, and confirmed in reference (13), and by tests conducted in this work.

4.2 Casting

Several proportions of resin and hardener were tried, and a final mixture of ten parts of hardener per hundred parts of resin (in weight) was adopted for all lab tests. The casting procedure and environmental conditions were always duplicated as closely as possible to ensure maximum consistency of results.

All mixtures were prepared in a room whose temperature was held at 75°F ± 1°F. The amount of ARALDITE and hardener mixed was always the same, and followed the same sequence: 160 grams of ARALDITE were placed in a container whose total capacity was twice as much, while 16 grams of hardener were measured in a different smaller container. The reason for placing the resin and the hardener in two different containers, rather than adding the hardener directly to the resin (or vice versa), was to avoid partial curing of the mixture during the process, which actually happened the first time the mixture was made. Two different containers allowed enough time for a careful and accurate measurement of both resin and hardener. The disadvantage of this procedure is that part of the hardener will remain on the walls of the container, producing a proportion of ingredients other than expected. This remainder was measured repeatedly, giving an average of 0.63 grams. An extra amount of hardener equal to this average was added to the theoretical 16 grams, and a check of the actual waste was subsequently carried out, giving the real proportion used for every particular case. These values fluctuated from 9.97 to 10.03%, when a proportion of 10% was desired.

Once the hardener was poured into the resin, the mixture was stirred vigorously for one minute, and then centrifuged for two minutes at about 1500 rpm.

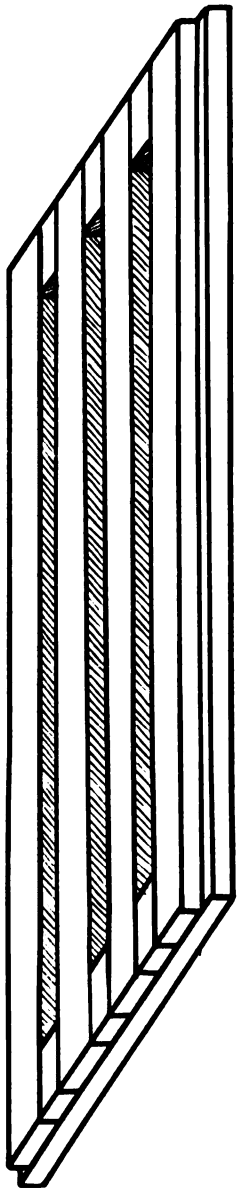

Figure 4.1.--Arrangement of molds to cast three specimens at a time.

Both the casting and the curing of the samples were done in the same room where all the tests were run. This room was kept at constant temperature of 80.5°F, with a fluctuation of ± 0.5°F. The relative humidity fluctuated from 40 to 60 per cent.

The molds were made of aluminum, and consisted of machined, prismatic bars resting on a heavier base, and arranged in such a way as to produce specimens 3/4" x 1" x 22" in size (Figure 4.1).

As mold release, three different products were used with no apparent difference: Silicone Release Agent, manufactured by Dow Corning Corporation, Midland, Michigan; FreKote 33 Release Agent, FreKote, Incorporated, Boca Raton, Florida; and Johnson Paste Wax, Johnson and Son, Incorporated, Racine, Wisconsin.

Before pouring the mixture, the mold was levelled to obtain a bar with uniform height, and clamped to avoid any leakage. Once the mixture was poured, the mold was covered to protect the sample from dust. The sample was kept in the mold for seven days, at the end of which the different pieces of the mold were released. An effort was made not to cause any disturbance of the sample.

If the sample was to be used in a creep test, end-pieces (Figure 4.3) were attached to its ends to provide supports, and to enable the application of end moments.

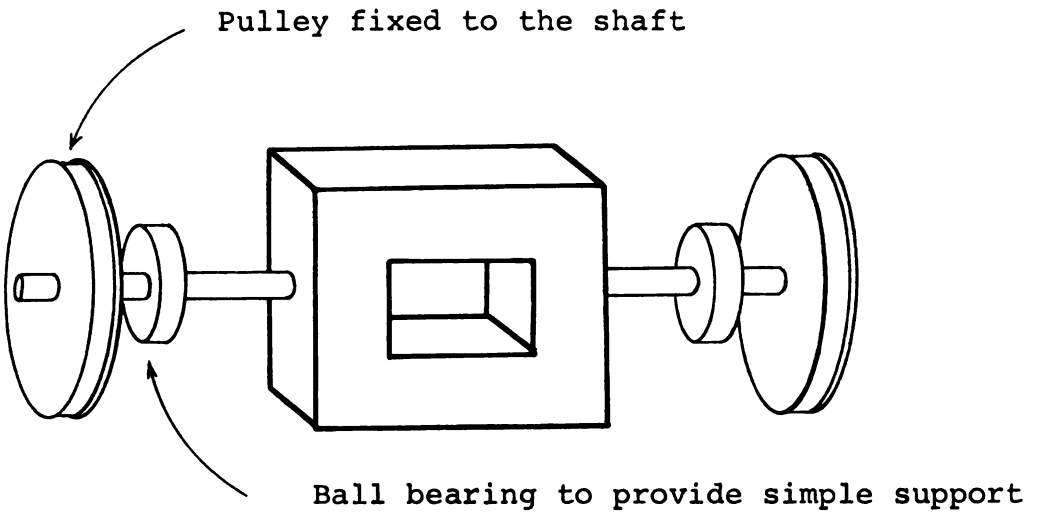

Figure 4.2.--End-piece

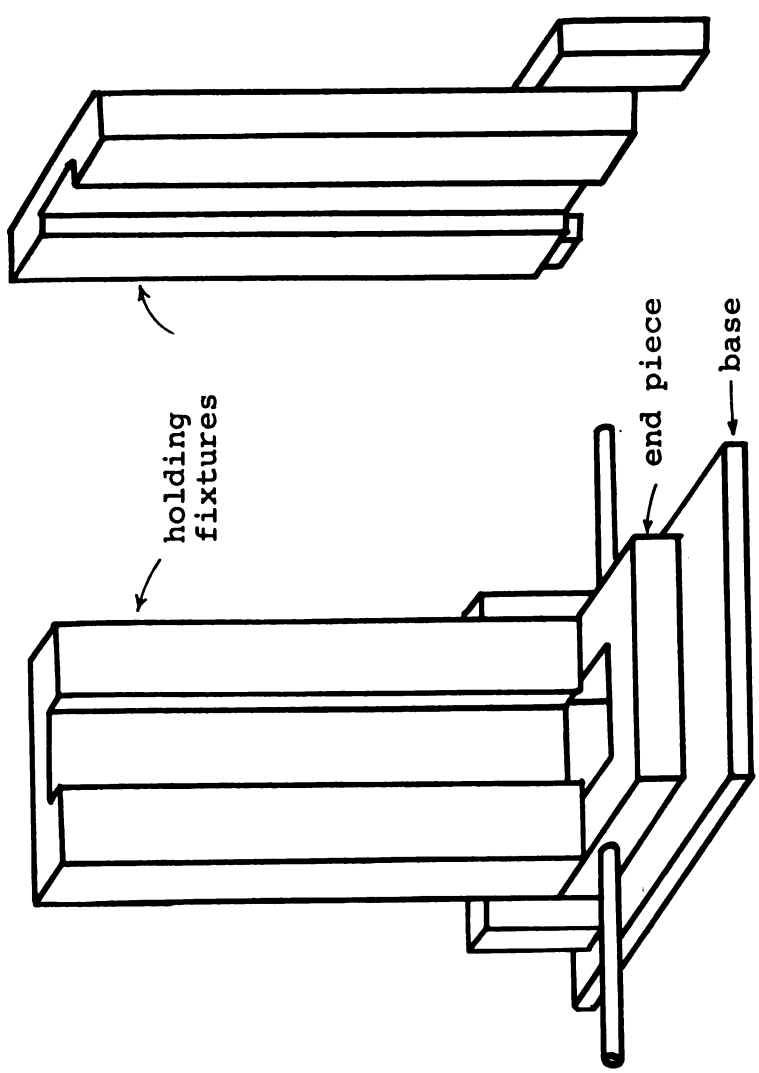

Figure 4.3.--Holding fixture.

In order to properly center the end pieces, and place them in a plane normal to the sample axis, a holding fixture (Figure 4.3) was used. The final beam model ready to be used in a creep test can be seen in Figure 4.4.

For frame models, the triple mold of Figure 4.1 was used. After one week of curing, the ends of the three bars were mitered and welded together. For this purpose, the pieces of Figure 4.1 and Figure 4.4 were combined to support the frame, while the joints were welded, as shown in Figure 4.5.

4.3 Creep Tests

The creep tests consisted of measuring the middle span deflections of a simple supported beam under equal constant bending moments, applied at the supports.

The following equipment was used:

1. Beam mounted on end-piece (Figure 4.5), with two inch diameter pulleys, from which a given weight could be hanged, producing the desired end bending moment.

2. Containers with lead pellets were used as loads. In this way, any arbitrary weight could be chosen, including the effect of hangers.

3. A Starret dial indicator was used to measure the middle span deflections. Some of the dial characteristics are as follows: range 0.4"; graduation 0.0001"; minimum load to overcome internal resistance 0.062 pounds; spring constant 0.0063 pounds per inch.

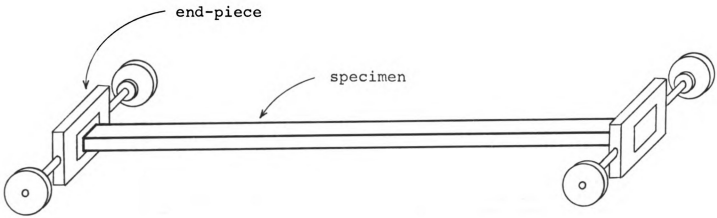

Figure 4.4.--Sample ready to be used in a creep test.

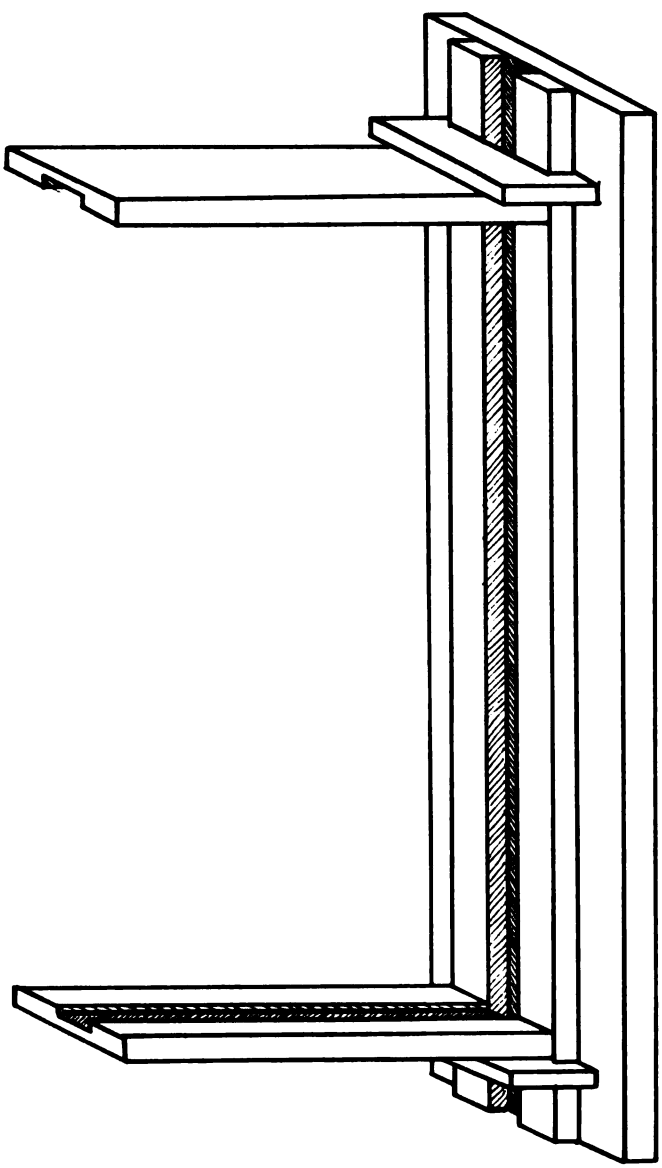

Figure 4.5.--Arrangement for welding of frame joints.

4. To measure time, use was made of an ordinary electric clock (Westclox), and a digital electric timer (model T-101), manufactured by Nuclear Instrument and Chemical Corporation, Chicago, Illinois. This timer measured hundredths of a minute, and had a range of 999.99 minutes. After this number was reached, the counting would start from zero again.

5. Finally, a hydraulic jack was used to apply the loads. A 2" x 6" x 30" piece of lumber was attached to the head of the jack. Before starting the test, the head of the jack was raised, and two weights, resting on the piece of lumber, were centered under the points of application and hung from the pulleys. A slow uniform downward motion of the jack was obtained by means of a control valve. A ballast of 56 pounds (two lead bricks) helped to further stabilize the motion and reduce the change of velocity while the load was transferred from the jack to the test model. In this way the load was applied at both ends uniformly and without significant impact effect.

Figure 4.6 shows the general set-up of a specimen under a creep test.

The help of a second laboratory operator was used to better synchronize the zero time with the application of the load, and it proved to be especially useful in the reading of the deflections at intervals of time as short as 0.06 minutes. It was pointed out in Chapter III that

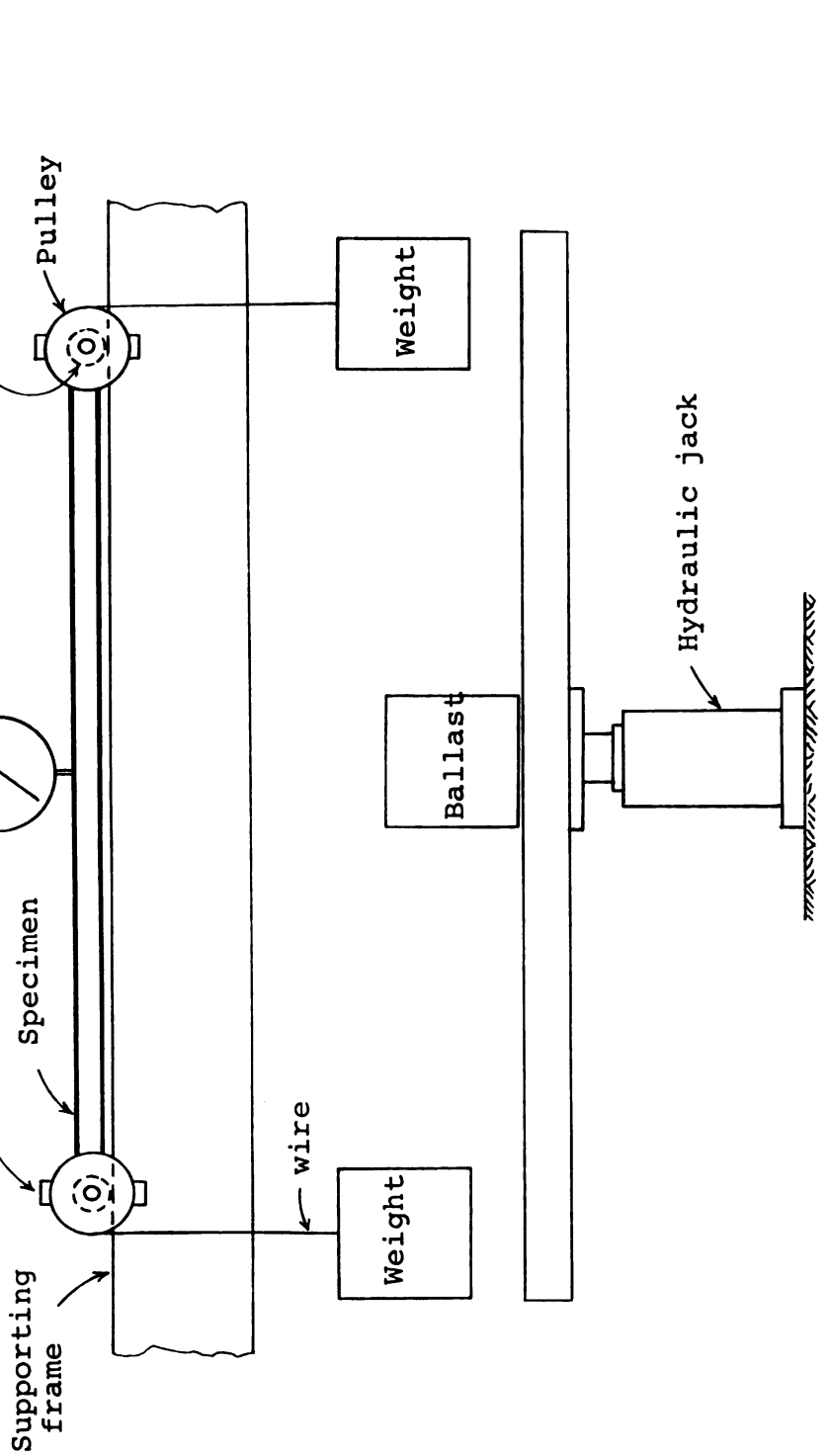

Figure 4.6.--Creep test set up.

to facilitate the evaluation of the relaxation modulus, very small intervals of time were to be taken for the first few minutes of the creep test.

Tests were run at different specimen ages. Finally, 35 days from the day of casting was adopted as the specimen age for all tests. This age was adopted partially arbitrarily, and partially influenced by the aging tests (see section 4.5).

To ensure that the values for the creep compliance were obtained within the linear range of the material, several tests were run under different loads. In fact, the maximum stress reached was 305 psi, a figure well below the 2500 psi claimed by the manufacturer* as linear range.

A better understanding of the results plotted in Figure 4.7 will follow from an estimate of the uncertainty involved in the tests. The effective beam length, from center to center of supports, was 19.25 ± 0.001", and the depth 0.75" ± 0.01". The effective length (pulley's radius plus hanging wire's radius) was 0.953" ± 0.001". The weights were measured in a scale with sensitivity of 0.01 lb. The proportion of hardener to resin varied from 9.97% to 10.03%, which, according to the

---

*Technical Service Note, A/24UX-1, Structural Resins Department, CIBA Products Corporation, Kimberton, Pennsylvania, 1969.

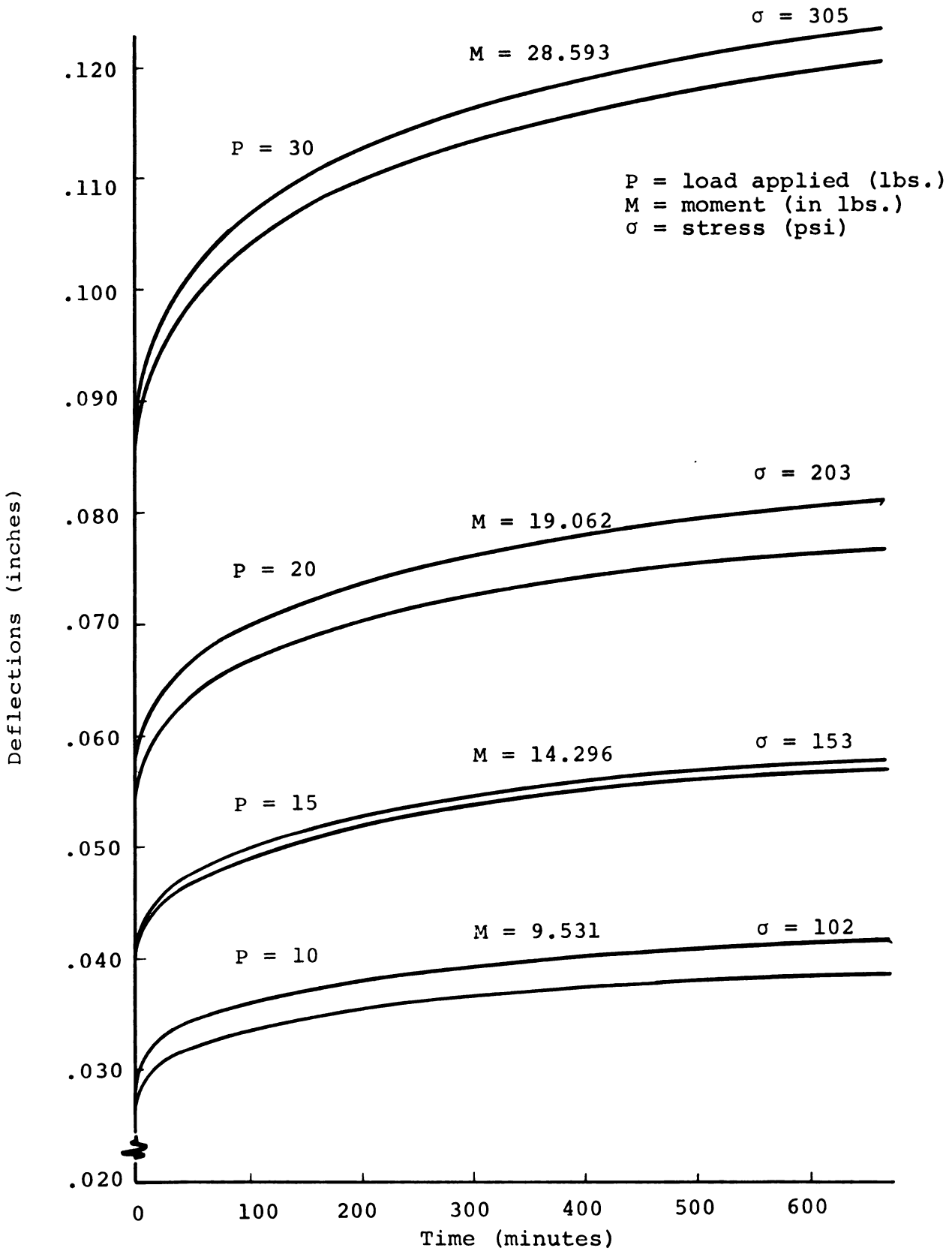

Figure 4.7.--Middle span deflections on creep tests.

manufacturer's literature, would mean a fluctuation of ± 1% of the mixture's stiffness.

Now an estimate of the uncertainty is readily available. The middle span deflection of a simply supported beam under equal concentrated end moments is given by

$$\Delta = \frac{ML^2}{8EI} \tag{4.1}$$

or else

$$\Delta = \frac{3WRL^2}{2Ebh^3} \tag{4.2}$$

where W is the hanging weight; R, the lever length; E, the Young's modulus; b, the beam width, and h, the beam depth.

Taking logarithms of both sides of Equation (4.2), changing the negative signs to positive (2), and differentiating, one obtains

$$\frac{d\Delta}{\Delta} = \frac{dW}{W} + \frac{dR}{R} + 2\,\frac{dL}{L} + \frac{dE}{E} + \frac{db}{b} + 3\frac{dh}{h} \tag{4.3}$$

where each quotient gives the relative uncertainty. Assigning numerical values to the right-hand side, Equation (4.3) becomes

$$\frac{d\Delta}{\Delta} = 0.061 \tag{4.4}$$

This means that the uncertainty of the values for the deflections is ± 6%, which more or less fits the results shown in Figure 4.8.

4.4 Creep Compliance Values

The deflections plotted on Figure 4.7 gave rise to different sets of values for the creep compliance. These values were averaged, and plotted on a semilogarithmic paper. A curve was drawn to best fit the tendency of the points plotted, and the values read from the curve were adopted as the "true" values of the creep compliance (see Figure 4.8).

The justification of this procedure lies, first of all, on the fact that in any measurement, the average of the different observations is the best estimate of the true value (2). Then, in this case, the scale selected in the semi-logarithmic paper to plot the mean values obtained for the creep compliance, had the same sensitivity as the dial gauge used to read the deflections, i.e., four significant figures.

The values read from the curve of Figure 4.8 appear tabulated on Table 2.7 together with the corresponding values of the relaxation modulus used in the numerical examples of frame analysis presented in Chapter V.

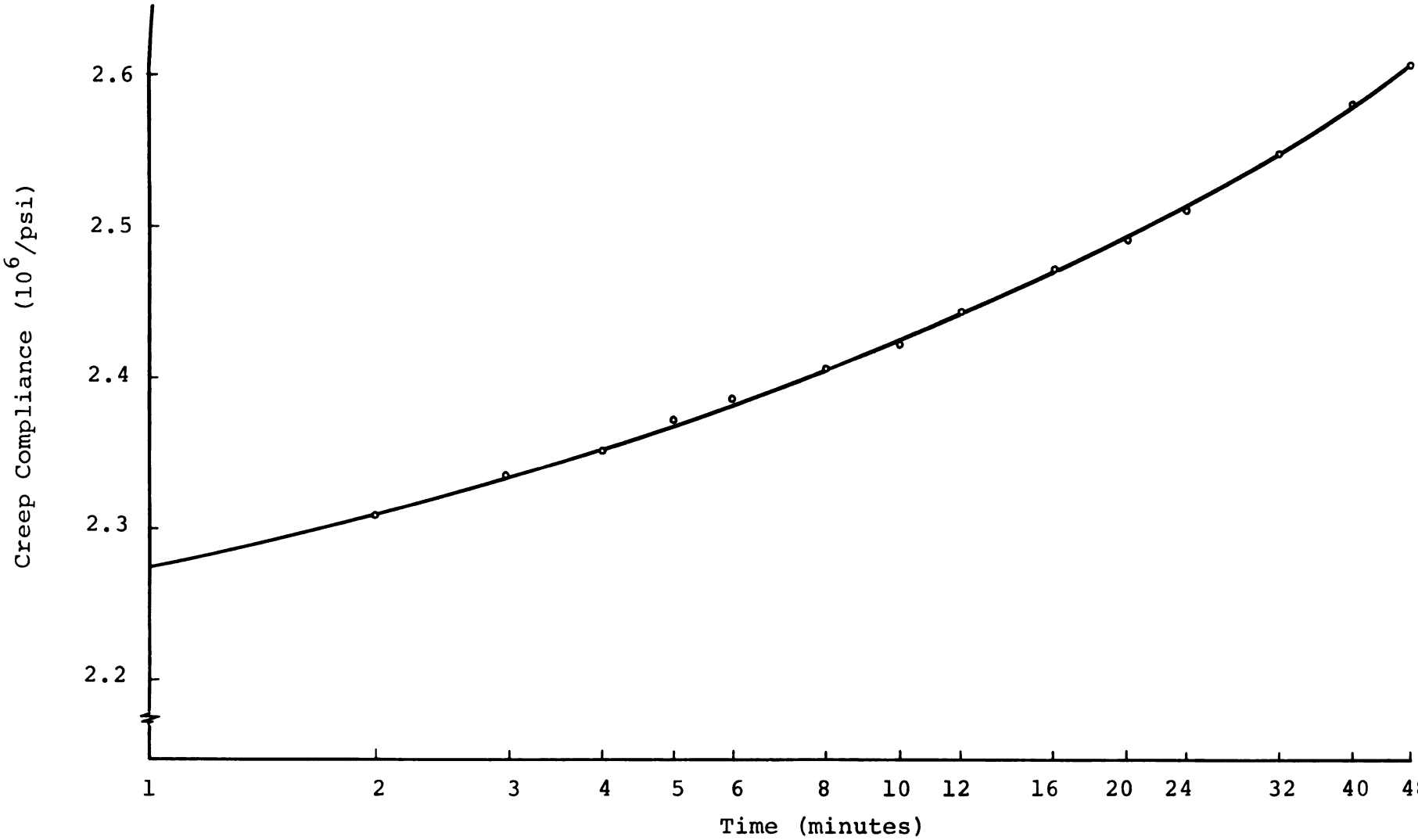

Figure 4.8 (Part I).--Creep compliance curve (Semilog).

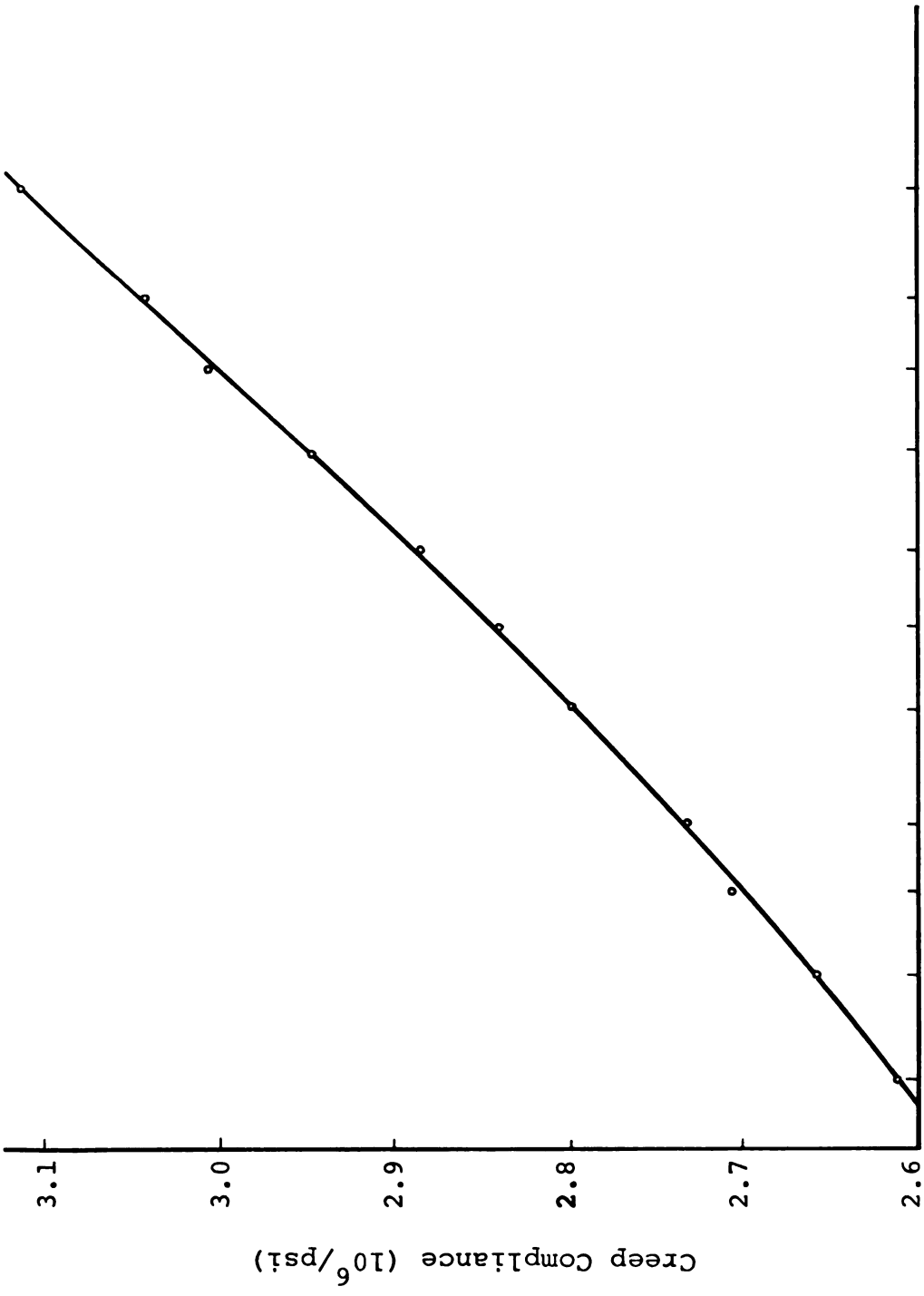

Figure 4.8 (Part II).--Creep compliance curve (Semilog).

4.5 Aging Tests

Two samples were tested a number of times at different ages to determine the curing process, the aging or the strengthening of the samples as they grow older. Although different results were obtained in the different tests, as can be seen in Figures 4.9 and 4.10, the tests cannot be considered conclusive, since there could be a number of factors, other than age, affecting the stiffness of the material.

An aging test, isolating age from all other possible causes, may prove useful, but in the present case would be beyond the scope of this study.

4.6 Frame Tests

Three different plane portal frames were made and tested. All were made up of rectangular bars with cross section of 1" x 3/4". They will be referred to as Frame 1, Frame 2 and Frame 3. Frame 1 was a rigid frame fully clamped at both supports, and tested under loads of 2 and 10 pounds. A sketch of the general set-up is shown in Figure 4.11. Frame 2 was essentially like Frame 1, with the beam two inches longer, and loads of 5 and 15 pounds, instead of 2 and 10, respectively. Frame 3 had one support clamped, and the other hinged, and was tested for 2 and 10 pounds as sketched in Figure 4.12.

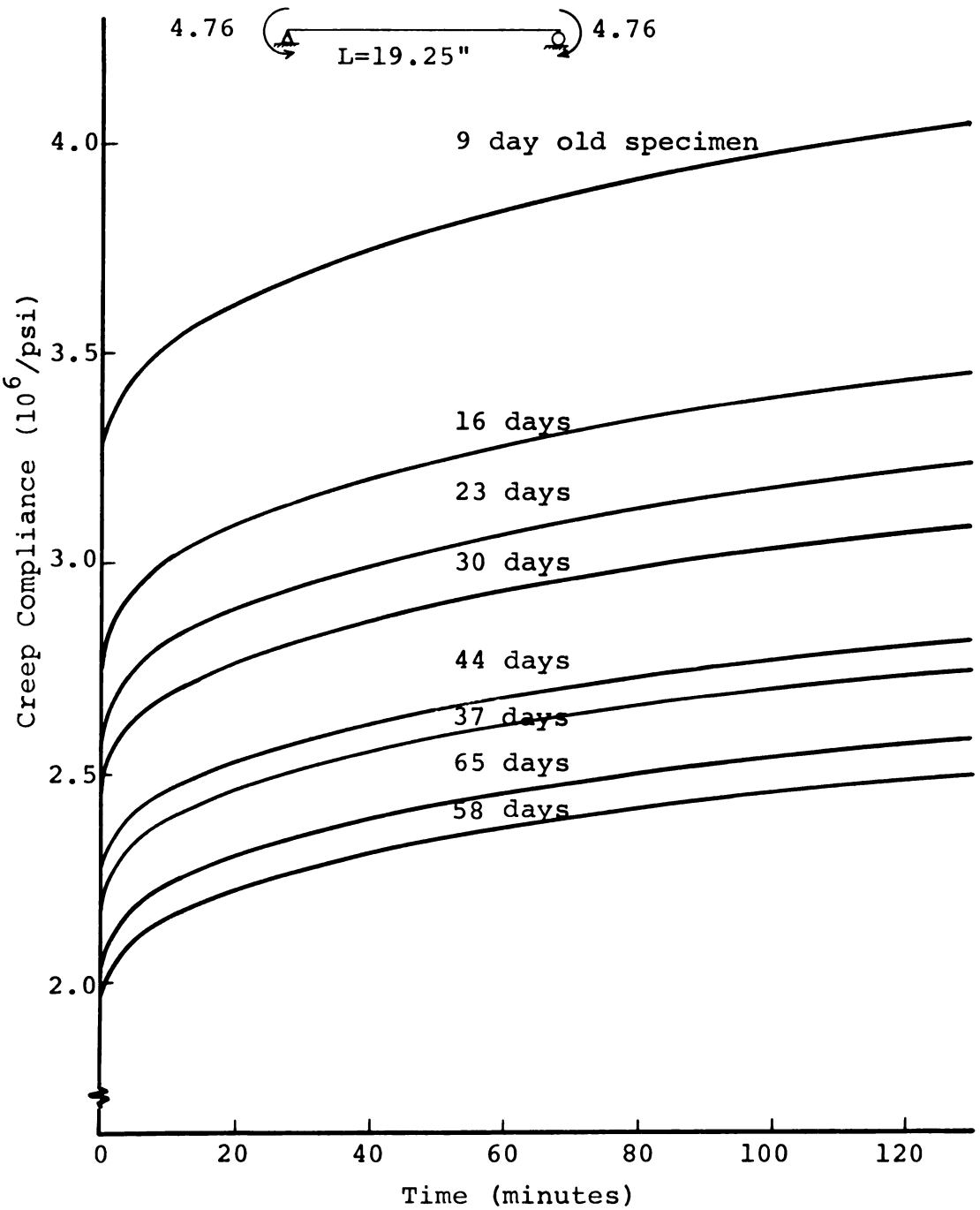

Figure 4.9.--Aging test. Simply supported beam.

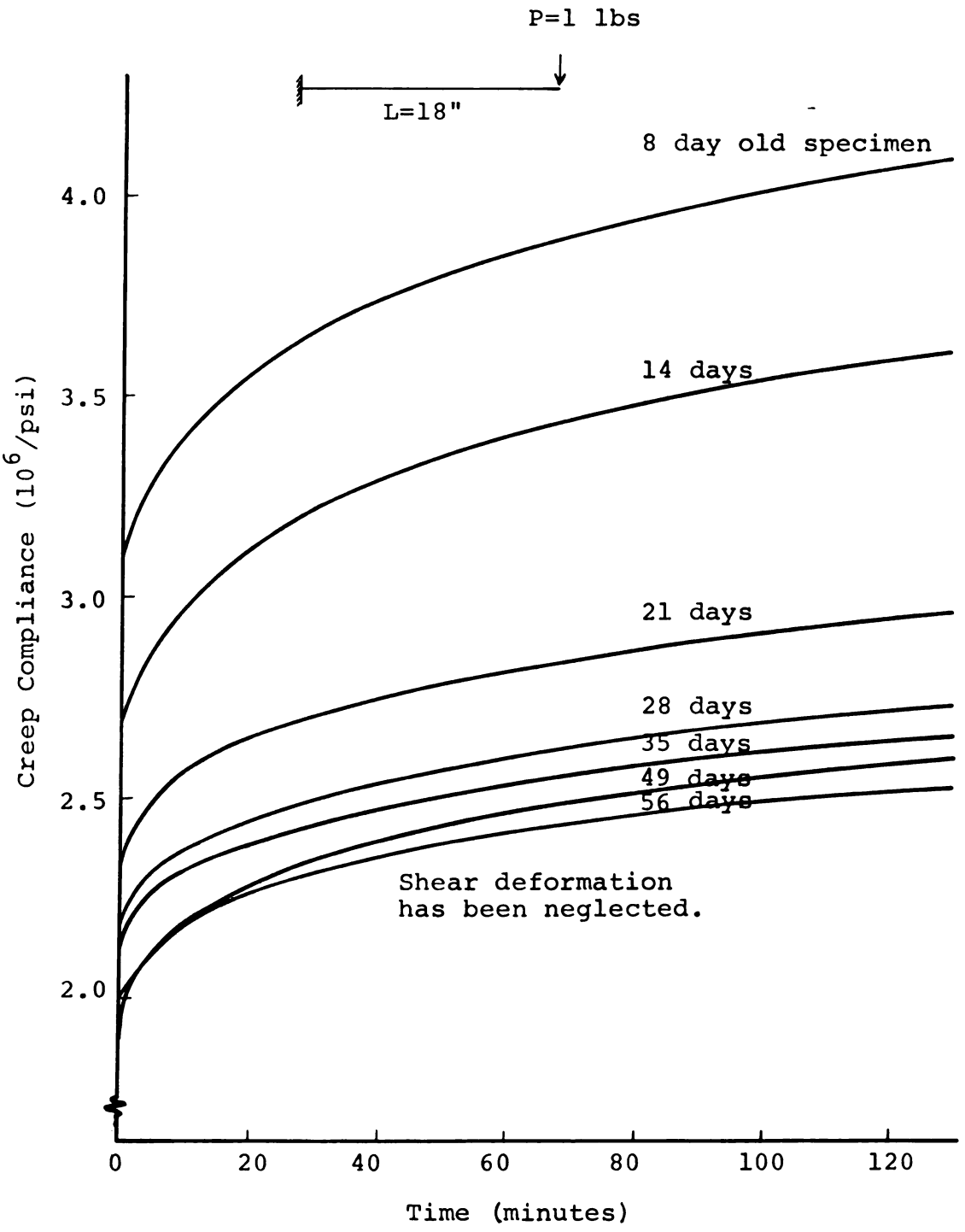

Figure 4.10.--Aging test. Cantilever beam.

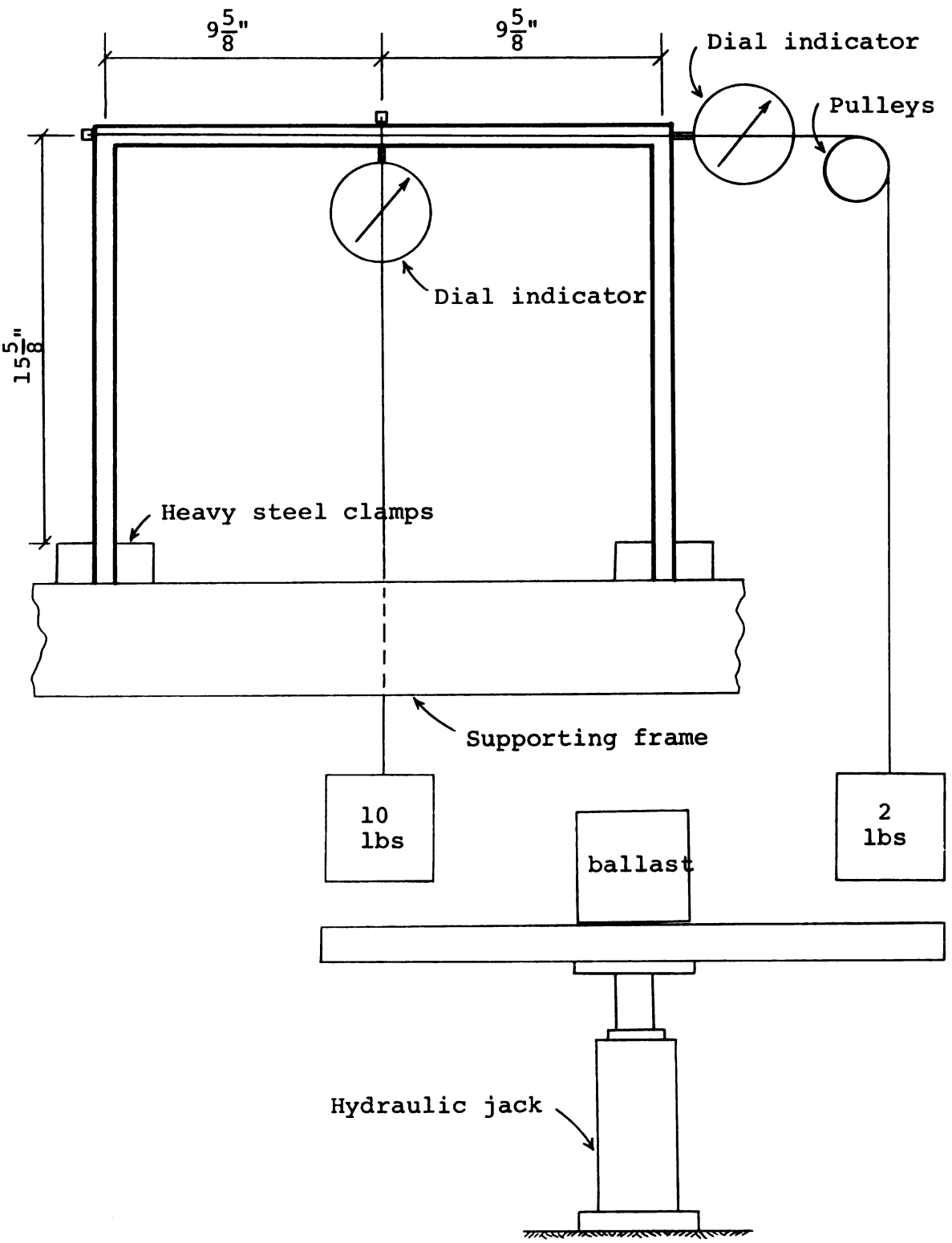

Figure 4.11.--Frame 1.

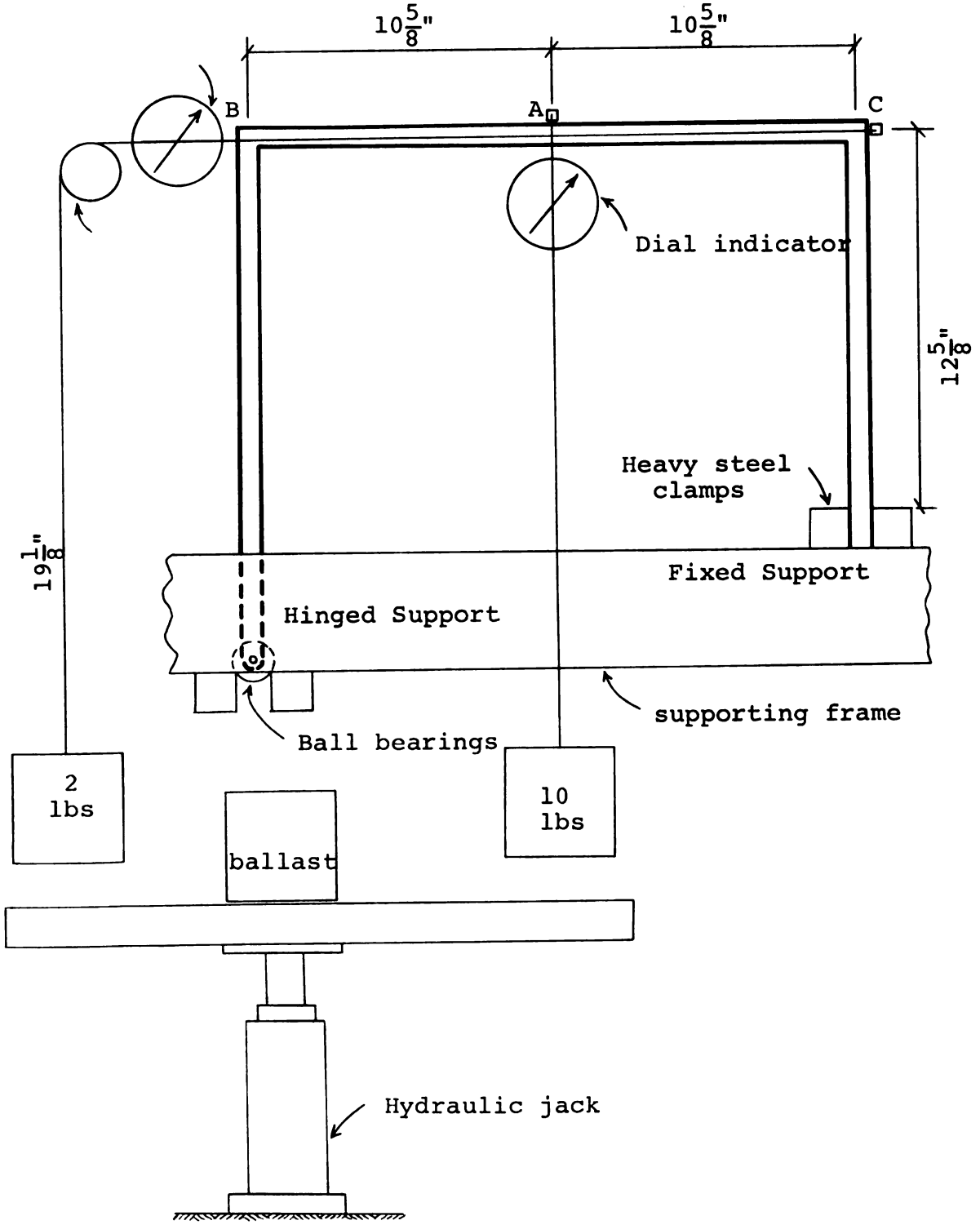

Figure 4.12.--Frame 3.

The vertical load was hung directly from the top middle point of the beam, while for the horizontal load two pulleys mounted on ball bearings were used. The loads, as in all other tests, were applied with the help of a hydraulic jack to avoid impact, and reduce to a minimum the effects of acceleration.

The tests were conducted when the frames were 35 days old, and the readings were spread to follow the pattern shown in the t-axis of Figure 3.6. As before, the help of a second operator was used to synchronize the zero time with the application of the loads.

CHAPTER V

RESULTS AND DISCUSSION

5.1 Introduction

In the first part of this chapter, results from the various methods used in this study will be presented and compared. The second part will consist of a general discussion, together with some conclusions.

5.2 Comparison of Relaxation Modulus Values

Figure 5.1 shows two curves obtained for the relaxation modulus values for the epoxy resin used in the lab tests of this work.

Curve 1 was obtained by inverting the creep compliance values given by the Equation (2.56), using for the parameters the values obtained by LaPalm (13). Curve 2 was obtained by direct inversion of the laboratory results obtained in this work. More exactly, curve 2 is the inverse of the creep compliance curve of Figure 4.8, which is the average of the different laboratory results.

The discrepancy of both curves is of the order of 2%. This confirms the reproducibility of the material used

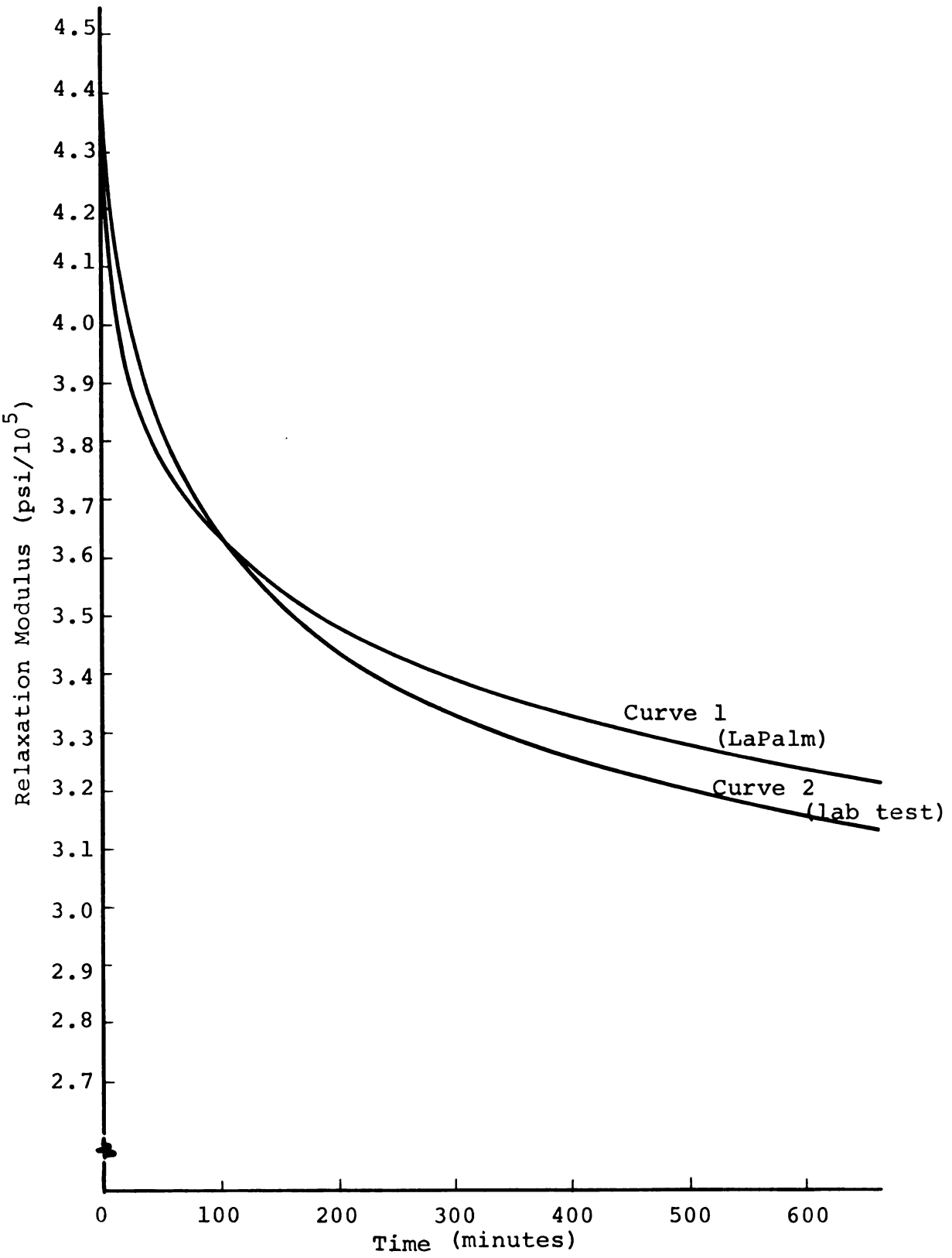

Figure 5.1.--Comparison of relaxation modulus curves.

for the tests, and adds support to the values obtained thus far for the relaxation modulus of such material.

5.3 Frame 1 Joint Displacements

Frame 1 is sketched in Figure 4.11. The vertical deflection of the middle span point, A, and the horizontal displacement of the right-hand corner, B, are plotted in Figures 5.2a and 5.2b, respectively.

Figure 5.2 shows the vertical deflections of midspan point A, and horizontal displacements of joint B of Frame 1. Each one of them is represented by three curves. Curve 1 represents results obtained from Equation (3.8) by means of the program VIELANAL, developed in Chapter III and listed in Appendix B. Curve 2 represents the quasielastic solution, i.e., at every time, t, an elastic solution is carried out by simply substituting the modulus of elasticity by the relaxation modulus E(t). Finally, curve 3 represents the displacements measured in the laboratory using models, as described in Chapter IV.

5.4 Frame 2 Joint Displacements

It was pointed out in Chapter IV that Frame 2 was like Frame 1, except for the horizontal member, which was two inches longer. Thus, Figure 4.11 can also serve as a sketch for Frame 2 if we read 10 1/2" instead of the 9 1/2" shown as the length for half of the horizontal member referred to.

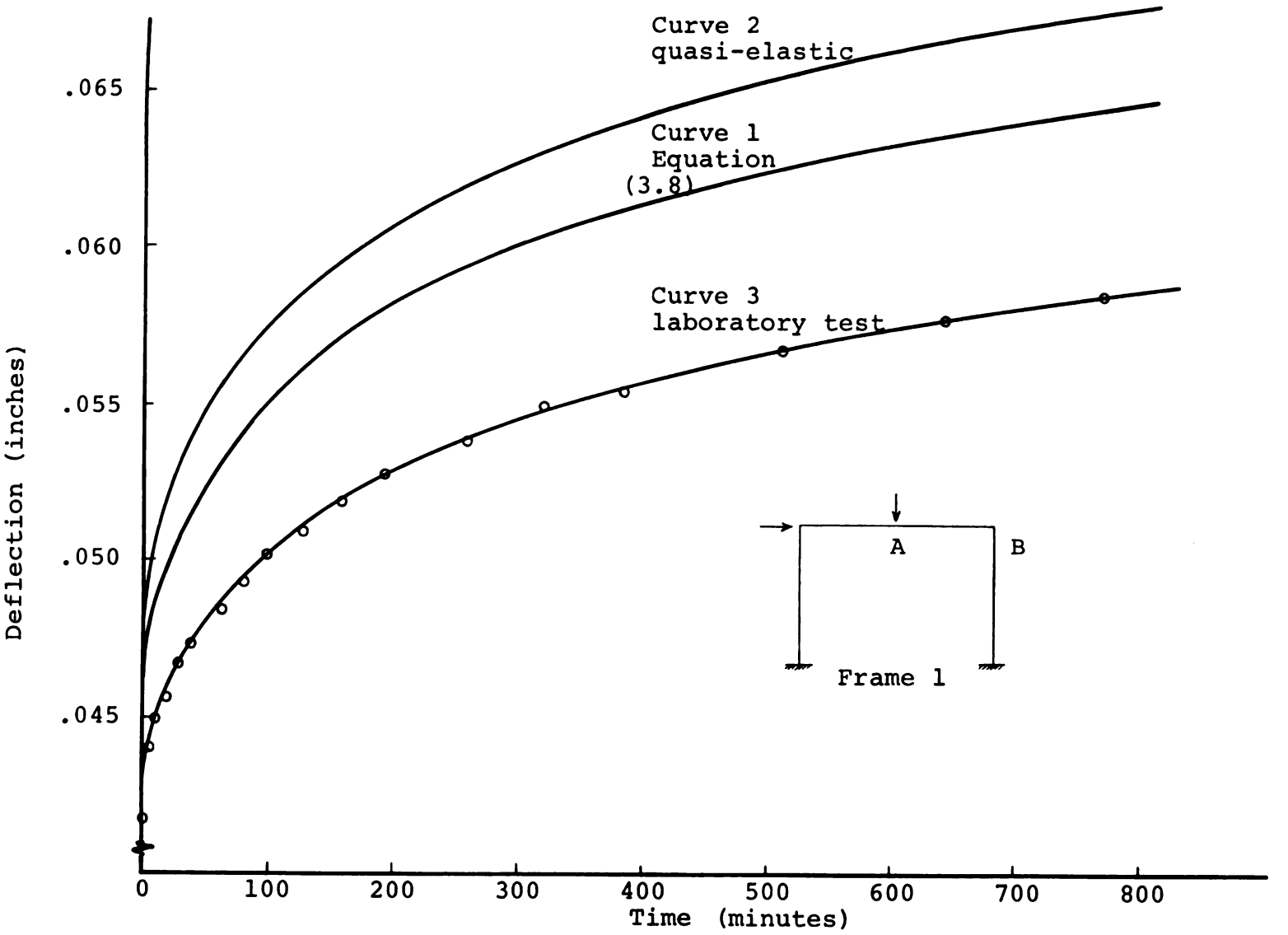

Figure 5.2a.--Vertical deflection of midspan point A of Frame 1.

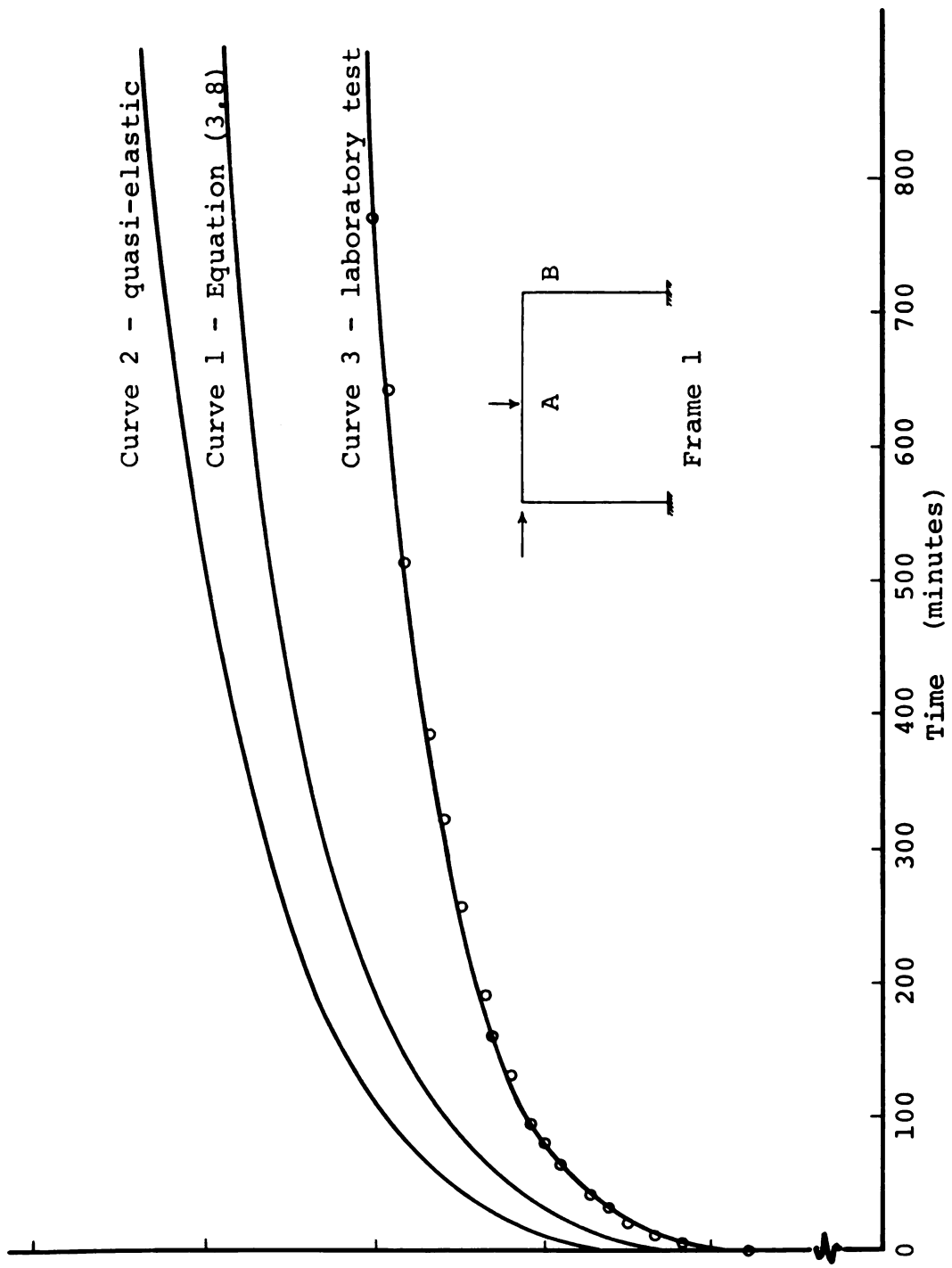

Figure 5.2b.--Horizontal displacement of joint B of Frame 1.

Figure 5.3 shows the joint displacements for Frame 2. The comments made in section 5.3 about curves 1, 2 and 3 can be applied here to Figure 5.3.

5.5 Frame 3 Joint Displacements

Frame 3 is sketched in Figure 4.12. Unlike Frames 1 and 2, it is unsymmetric. Also, one of the supports is hinged, while the other remains clamped.

Figure 5.4 represents the vertical deflection of the midspan point A, and the horizontal displacement of joint B. The comments about curves 1, 2 and 3 can also apply here.

At this point, a remark about frame stresses seems to be in order, since so far, nothing has been said about the range within which the frame tests have been conducted. For Frames 1 and 2 the maximum normal stresses occurred in the midspan point, A (see Figure 4.11), in both cases, and they were 335 psi and 364 psi, respectively. For Frame 3, the maximum normal stress occurred at the joint C (see Figure 4.12), and it was equal to 406 psi. Although these figures exceed the maximum stress value for which the material was tested in this study (305 psi, see Figure 4.7), the agreement of laboratory results with the numerical linear analysis causes the writer to feel that it is plausible to assume that the frame tests were run within the linear range of the material.

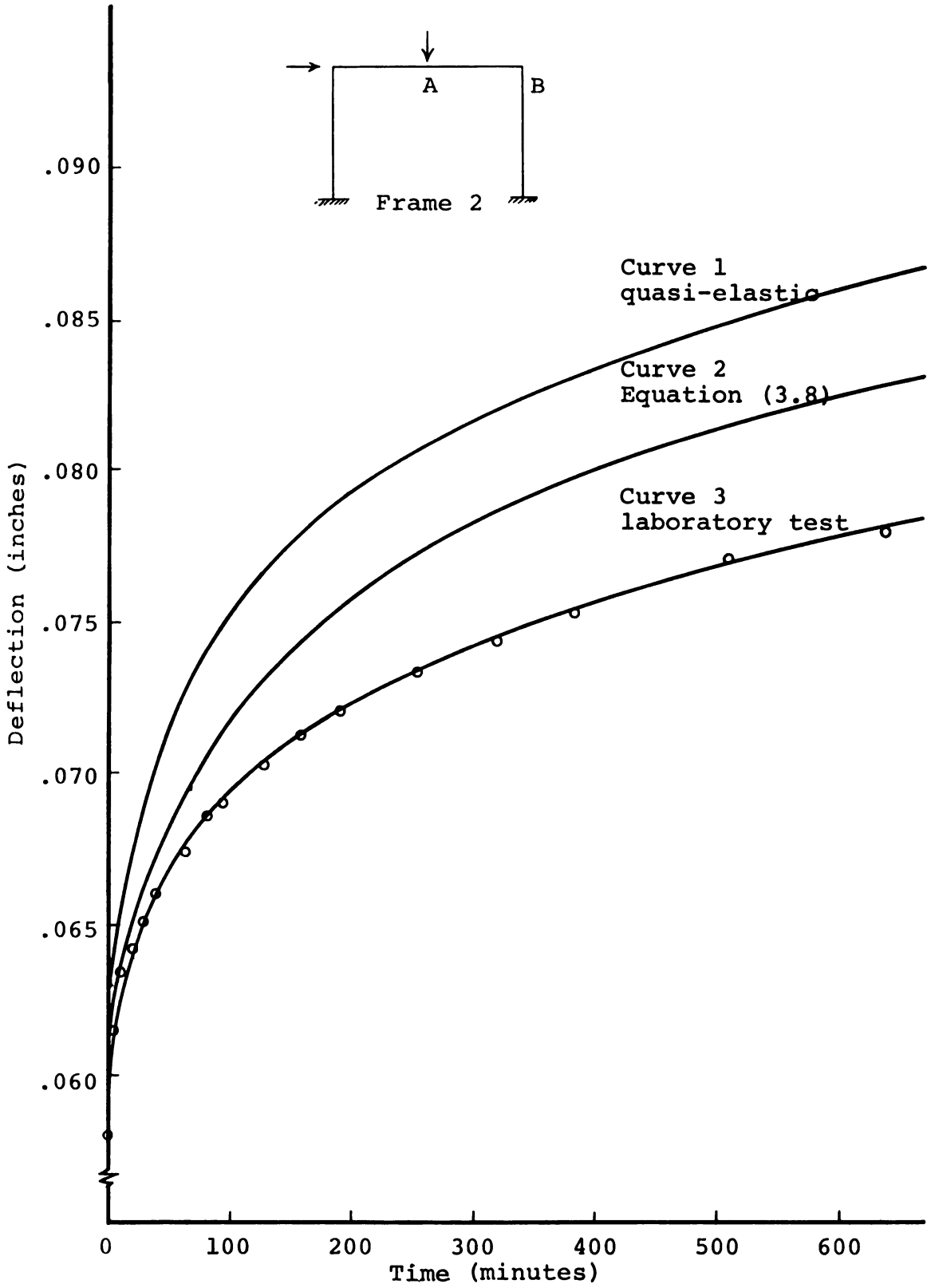

Figure 5.3a.--Vertical deflection of midspan point A of Frame 2.

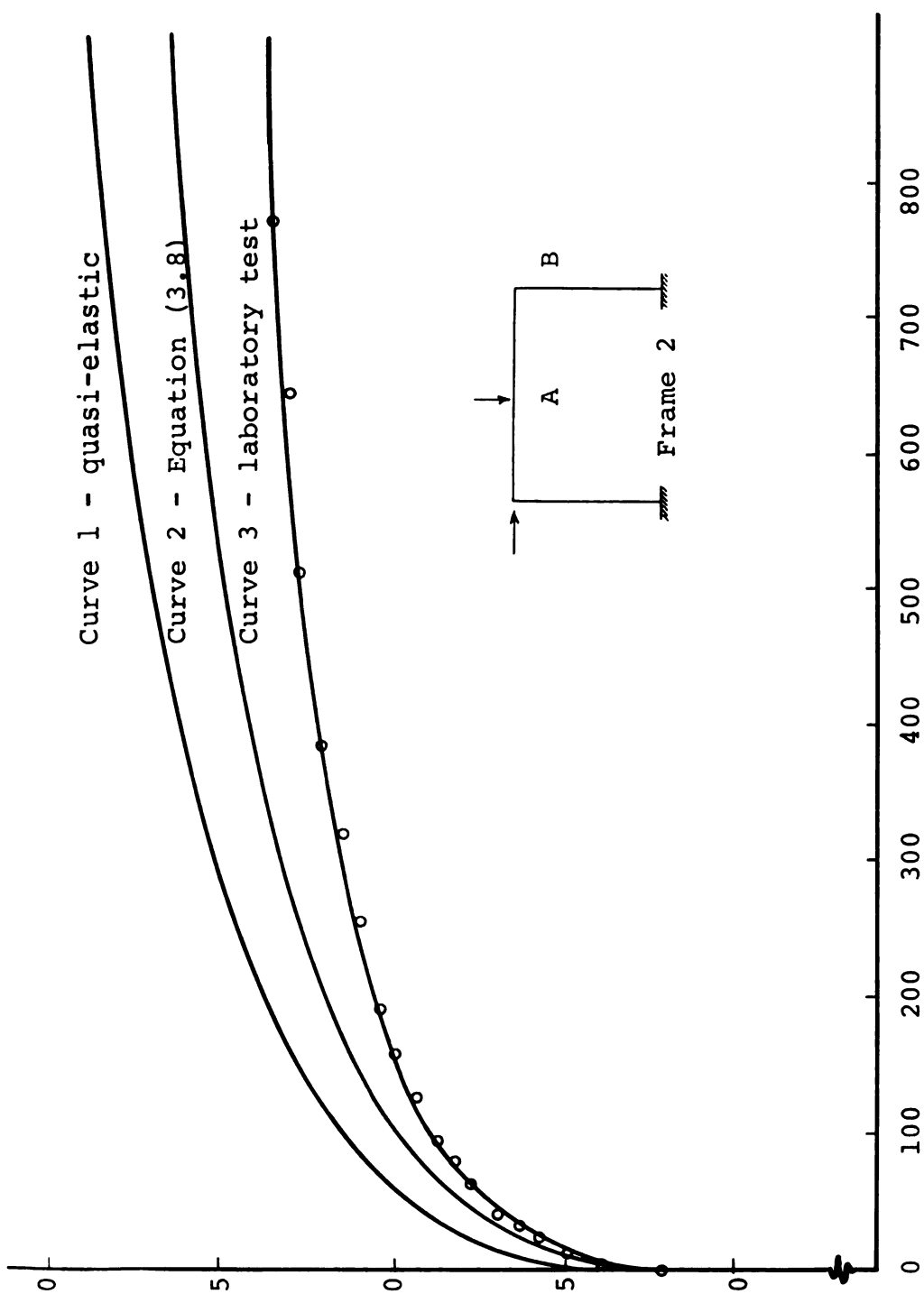

Figure 5.3b.--Horizontal displacement of joint B of Frame 2.

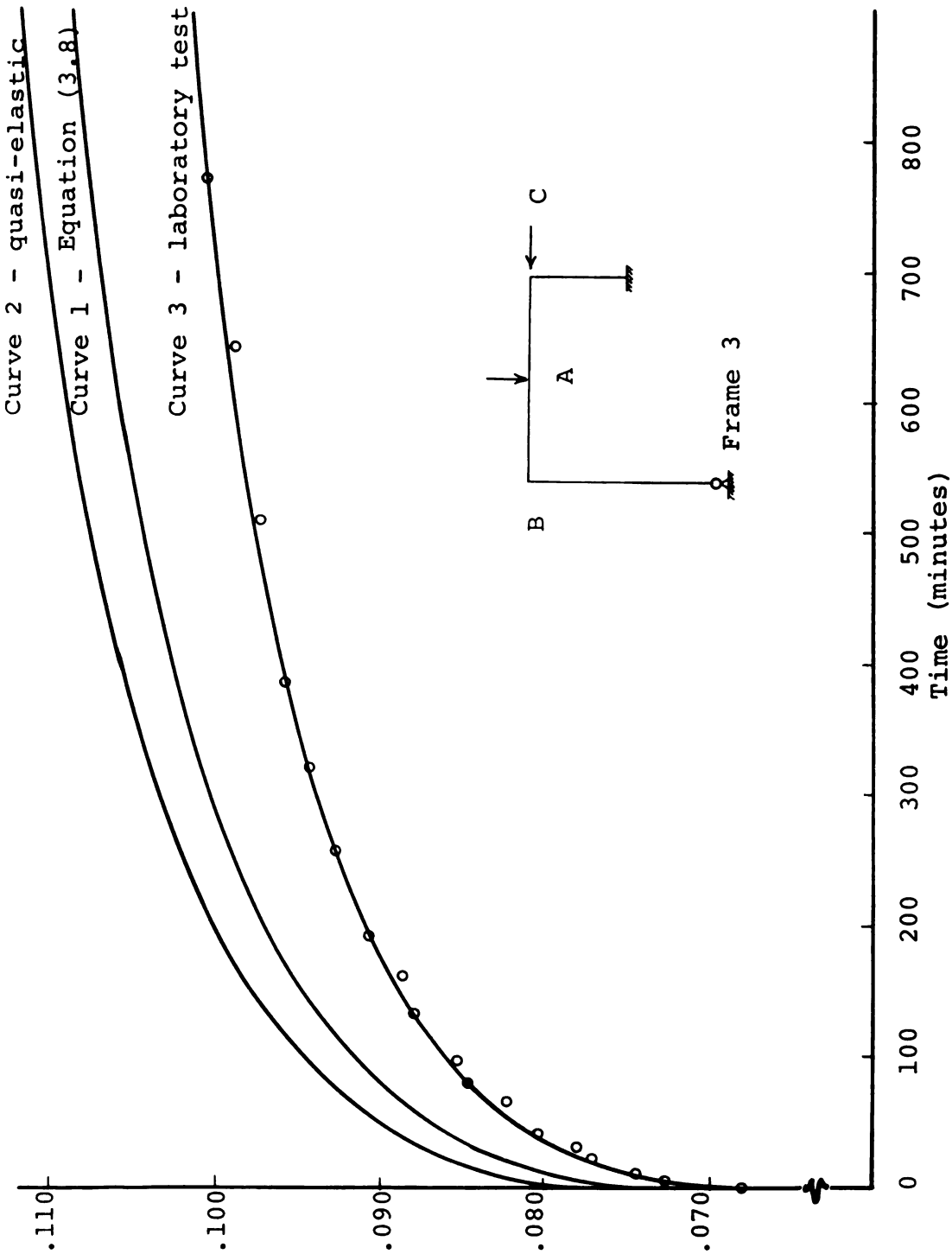

Figure 5.4a.--Vertical deflection of midspan point A of Frame 3.

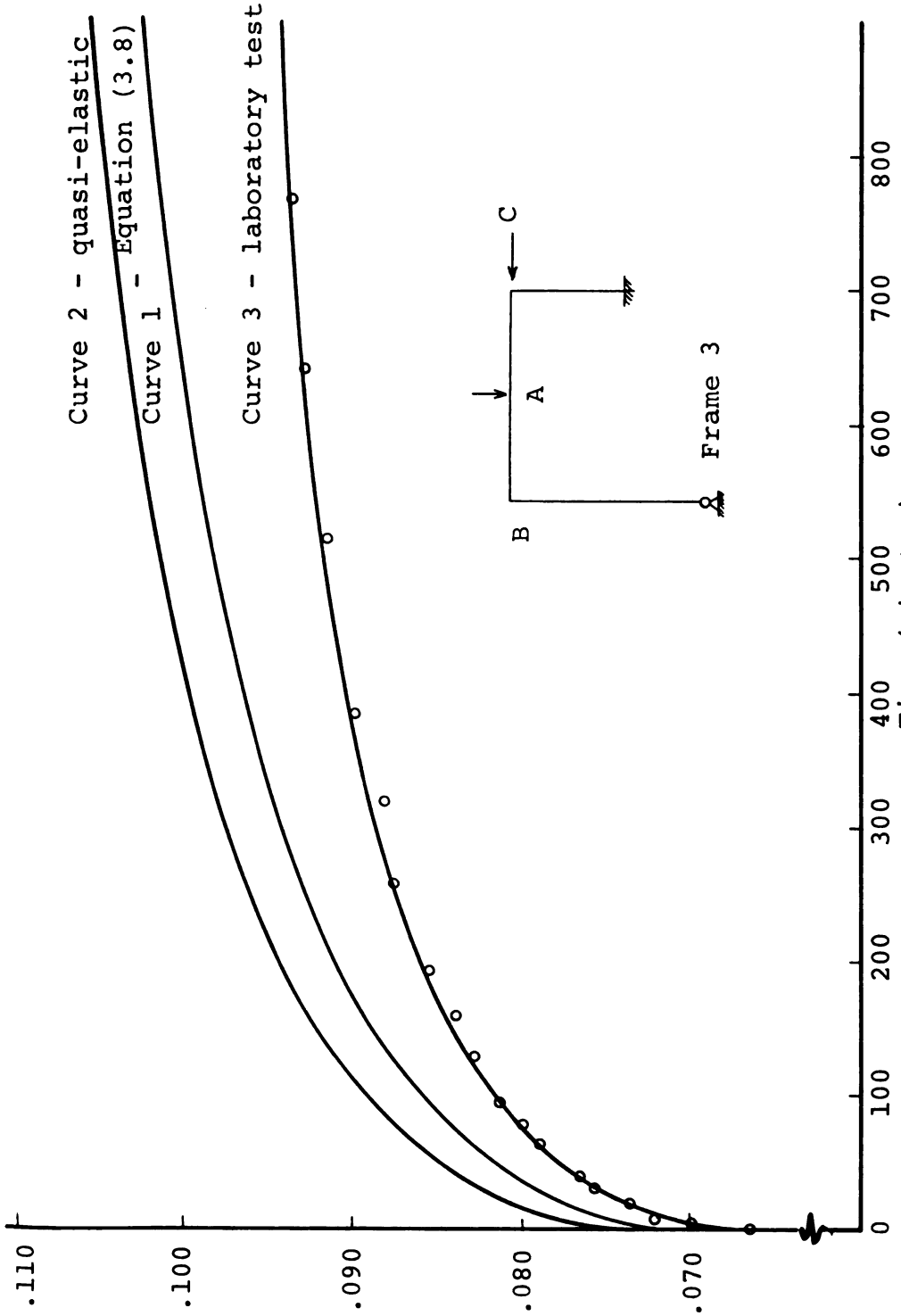

Figure 5.4b.--Horizontal displacement of joint B of Frame 3.

5.6 Epoxy Resin Used for the Laboratory Models

The epoxy resin used for laboratory models has a wide range for which the strains are proportional to the stresses. Also, Figure 5.1 shows that, within this linear range, the behavior of the resin is viscoelastic.

The material does not have a fixed stiffness in its early age. This means that, when comparing test results from different samples, attention should be given to the age of such samples. Figure 5.5 shows the tendency with which the resin stiffness increases with age. The curve was obtained from the values corresponding to 120 minutes shown in Figures 4.9 and 4.10. This is 120 minutes after application of load. The inverse of these deflections was multiplied by a reducing factor. This curve, based only on two different tests, does not pretend to be conclusive, but, as stated above, it shows the general tendency of the material stiffness increasing with age.

In the present work, the aging of the material during the test period was disregarded, since all loads were applied to the material at the same material age.

5.7 Laboratory Equipment

The laboratory equipment was simple but adequate. Still, a redesign of molds and end-pieces is recommended. The end-pieces should be designed as an integral part of the molds. This would avoid disturbances of the specimen

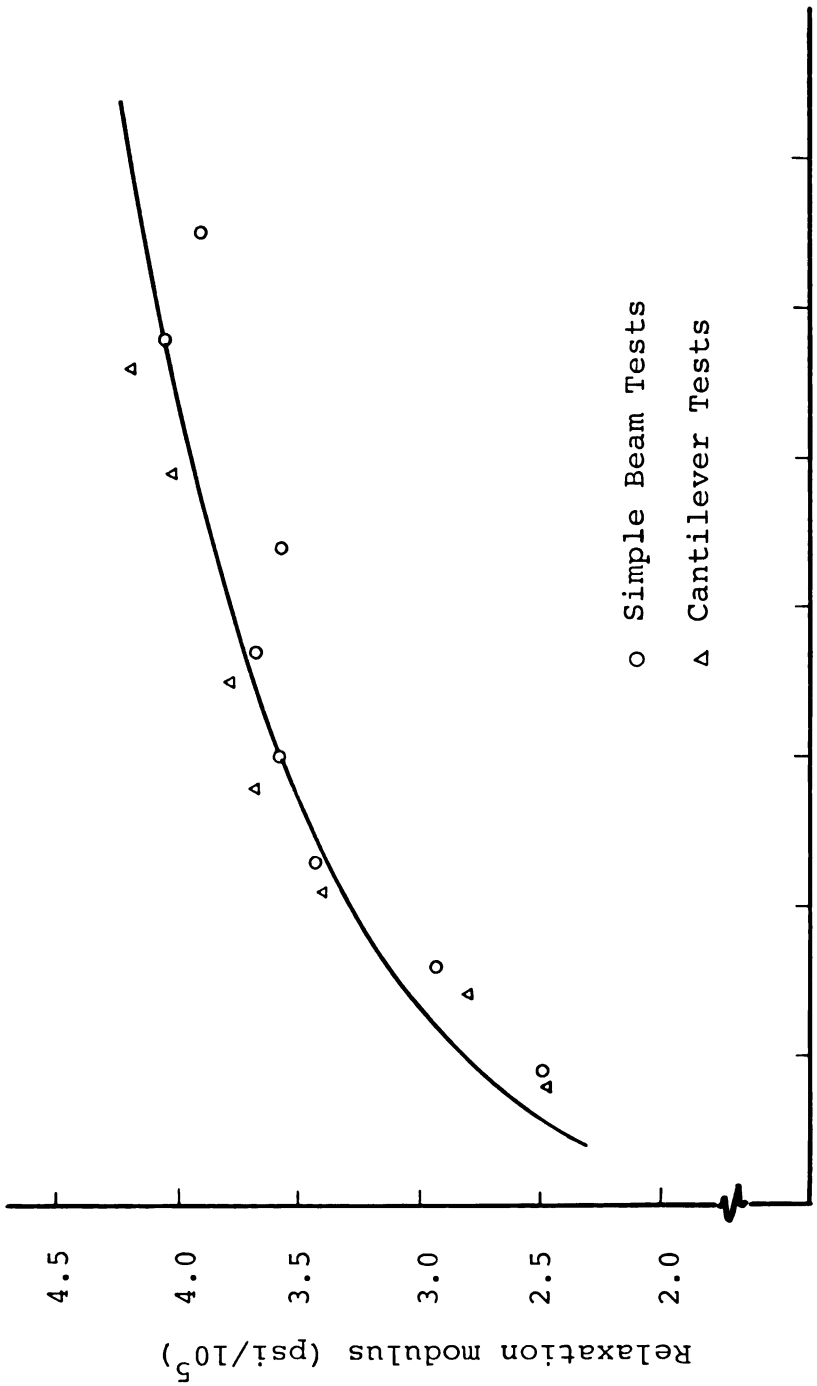

Figure 5.5.--Relaxation modulus increase with age.

while attaching the end-pieces, and, in addition, would provide more accuracy in the attachment of such pieces. Furthermore, the molds should be designed in such a way to allow the test to be set up before the molds are released. Finally, a set of screws could be used to allow the molds to be removed smoothly, leaving the specimen undisturbed and ready for the desired test without requiring any further handling.

5.8 Relaxation Modulus

The presence of oscillations of the lower bound for the values of the relaxation modulus (see Tables 2.3 and 2.4) still remains open to further study.

However, it has been shown that, by means of an adequate redefinition of time intervals, this difficulty can be overcome. In this way, we can invert creep compliance values to obtain the corresponding relaxation modulus without recourse to the Laplace transform. Furthermore, this method is applicable to creep values obtained from an algebraic formulation, as well as those obtained from discrete laboratory data.

A relaxation test is still desirable and recommended to prove the accuracy of both Equation (2.4) and Equation (2.5).

5.9 Matrix Analysis Formulation

In Chapter III a matrix analysis for framed structures was developed, and a digital computer program, VIELANAL (see Appendix B), was written. The results of this numerical solution differed from those obtained by models tested in the laboratory by discrepancies of the order of 10%.

In section 4.3 the uncertainty of the measurement of midspan deflections of a simple beam model was estimated to be of the order of 6%. In the case of a frame with three members, it seems reasonable to assume that this uncertainty will increase. Additional sources of error can be stated, such as improper set up, friction in the pulleys used for transmission of horizontal load, and, for Frame 3, friction in the hinged support. Finally, part of the 10% of discrepancy between the theoretical and experimental results has to be accounted for by the fact that the numerical analysis was an upper bound of the solution.

This program was based on Equation (3.3), which provides an upper bound to the governing Equation (3.2). By a simple change in indices, using E(0) instead of E(1) and (i+1) instead of (i), the program can be run for the lower bound given by Equation (3.4). However, this requires knowing the value of E(0), which is not readily available.

E(0) can be approximated from Equation (2.5), yielding

$$E(0) = \frac{1}{D(0)}, \tag{5.1}$$

where the value of D(0) would have to be obtained from extrapolation in the semilogarithmic curve of Figure 4.8.

In the present work, however, the extrapolation from the curve of Figure 4.8 is not well determined, due to lack of enough data near time equal to zero, producing little more than meaningless results.

The difficulty of obtaining the glassy properties of the material increases when we keep in mind that, while on the one hand, a step load at time zero is desired, on the other hand, the application of such load has to be smooth and gradual to avoid impact effect.

When the nonlinear geometry and the axial force effects were omitted (see Table 5.1), the joint displacements dropped about one per cent. It must be kept in mind, however, that the samples run in this study were kept under practically linear geometry conditions, to ensure linear behavior in the material. Under a heavier loading system, the discrepancy between linear and nonlinear geometry and thrust effects may be of relevant importance, and, therefore, further research in this area is recommended.

Figures 5.2 through 5.7 show that the matrix formulation developed in Chapter III, based on LaPalm's Equation (3.3), produces satisfactory results.

5.10 Number of Finite Parts per Member

To calculate the fictitious joint loading, a finite difference method was used. Table 5.2 shows the accuracy obtained and the computer time needed for a given number of equal parts into which a member is divided.

From Table 5.2 we can conclude that a choice of 10 or 15 parts per member may be considered economical and still accurate enough for most practical considerations.

TABLE 5.1.--Axial force effect on joint displacements.

I. Vertical deflection of midspan point A (see Figures 4.11 and 4.12) at time t = 1.

Frame	Axial Force Effect taken into Consideration	Axial Force Effect Neglected	Discrepancy
	in	in	%
1	0.0461	0.0459	0.5
2	0.0600	0.0597	0.5
3	0.0762	0.0755	1.0

II. Horizontal displacement of joint B (see Figures 4.11 and 4.12) at time t = 1.

Frame	Axial Force Effect taken into Consideration	Axial Force Effect Neglected	Discrepancy
	in	in	%
1	0.0318	0.0315	1.0
2	0.0327	0.0324	1.0
3	0.0717	0.0710	1.0

TABLE 5.2.--Number of finite parts taken per member, versus accuracy and computer time.

Number of Equal Parts	Computer Time* (seconds)	Accuracy** (%)
6	0.14	85.4
10	0.16	92.7
15	0.19	95.4
20	0.25	95.9
40	0.78	97.2
50	1.33	97.7

*CDC 3600 Digital Computer

**A fixed-end beam under a load equal to cos x was considered. The values obtained from the numerical analysis were compared with the exact solution.

CHAPTER VI

SUMMARY AND CONCLUSIONS

A matrix method for numerical analysis of framed structures made of linear viscoelastic materials has been presented. The solution method has been embodied in a computer program written in Fortran. This program has been tested for plane frames, with different supports conditions, in a CDC 3600 and in a CDC 6500 digital computer.

The analysis uses constant loads concentrated at the joints, as the actual external loading system. Then, as time increases, fictitious joint loads are computed and added to the actual external joint loads. The fictitious joint loads were derived from the deformation history of the structure. This was carried out by means of a finite difference method scheme.

In order to store the information needed from the past deformed configurations of the structure, a redefinition of time interval was used as many times as needed to cover any desired time span. This time interval redefinition is flexible, and can be modified and adapted to particular cases, according to the structure size, and computer store capacity.

In the examples worked in this study, small loads were used. The purpose of using small loads was two-fold. First, this assured working within the linear range of the material. Second, the joint displacements were kept small, reducing to a minimum the reaction of the internal spring of the dial indicator. This resulted in a case with small axial thrust and practically linear geometry. As a result, the nonlinear geometry and axial forces included in this study had negligible effects on the joint displacements and stresses of the frames. When the nonlinear geometry and axial forces effects were omitted, the lateral sway dropped only by 2%. Of course, for heavier loading, this discrepancy may increase considerably.

Laboratory tests were run with symmetric and asymmetric frames made of a linear viscoelastic material. The laboratory results were compared with those obtained from the numerical analysis with satisfactory agreement.

A computer program to evaluate the creep-relaxation inversion has also been presented. In this program, a redefinition of time interval was also needed. However, this redefinition differs in nature and purpose from the one used in the frame analysis.

The relaxation modulus values are obtained from the creep-compliance values without recourse to the Laplace transform. The creep compliance can be given either as a

general algebraic expression or as a set of discrete values, obtained from laboratory tests.

In conclusion, a matrix method of analysis for frames made of linear viscoelastic materials has been developed. This analysis is carried out without expressing the viscoelastic material properties in terms of spring and dashpot models. Furthermore, this method is general, and parallels those existing for elastic structures under static constant loadings.

Future extensions of this study could include:

1. Effect of nonlinear geometry and axial thrust for structures under large deflections.
2. Nonlinear viscoelastic materials.
3. Loading that changes with time.
4. Dynamic analysis.

LIST OF REFERENCES

LIST OF REFERENCES

1. Alfrey, T., "Mechanical Behavior of High Polymers," High Polymers, Vol. VI, Interscience Publishers, Inc., New York, 1965.

2. Baird, D. C., Experimentation: An Introduction to Measurement Theory and Experiment Design, Prentice-Hall, Inc., Englewood Cliffs, New Jersey, 1962.

3. Battista, O. A., Fundamentals of High Polymers, Reinhold Publishing Corporation, New York, 1958.

4. Bland, D. R., The Theory of Linear Viscoelasticity, Pergamon Press, Oxford, 1960.

5. Flügge, W., Viscoelasticity, Blaisdell Publishing Company, Waltham, Massachusetts, 1967.

6. Fröberg, C. E., Introduction to Numerical Analysis, 2nd edition, Addison-Wesley Publishing Company, Reading, Massachusetts, 1969.

7. Fung, Y. C., Foundations of Solid Mechanics, Prentice-Hall, Inc., Englewood Cliffs, New Jersey, 1965.

8. Gere, J. M., and W. Weaver, Analysis of Framed Structures, D. Van Nostrand Company, Inc., Princeton, New Jersey, 1968.

9. Gurtin, M. E., and E. Sternberg, "On the Linear Theory of Viscoelasticity," Archive for Rational Mechanics and Analysis, Vol. 11, 1962, pp. 291-356.

10. Hall, A. S., Woodhead, R. W., Frame Analysis, 2nd edition, John Wiley and Sons, Inc., New York, 1965.

11. Hoff, N. J., "Approximate Analysis of Structures in the Presence of Moderately Large Creep Deformations," Quarterly of Applied Mathematics, Vol. XII, 1954, pp. 49-55.

12. Hult, J. A. H., Creep in Engineering Structures, Blaisdell Publishing Company, Waltham, Massachusetts, 1966.

13. LaPalm, G. E., "The Creep Buckling of Viscoelastic Beam-Columns," A Thesis Submitted to the Faculty of Purdue University, January, 1968.

14. Odqvist, K. G., "Applicability of the Elastic Analogue to Creep Problems of Plates, Membranes and Beams," Creep in Structures, Colloquium, Stanford University, Academic Press Inc., Publishers, New York, 1962.

15. Patel, S. A., and Venkatraman, B., "On the Creep-stress Analysis of Some Structures," Creep in Structures, Colloquium, Stanford University, Academic Press Inc., Publishers, New York, 1962.

16. Salvadori, M. G., and M. L. Baron, Numerical Methods in Engineering. 2nd edition, Prentice-Hall, Inc., Englewood Cliffs, New Jersey, 1962.

17. Timoshenko, S. P., and J. M. Gere, Theory of Elastic Stability. 2nd edition, McGraw-Hill Book Company, New York, 1961.

18. Wang, Chu-Kia, Matrix Method of Structural Analysis, 2nd edition, International Textbook Company, Scranton, 1970.

19. Williams, M. L., "Structural Analysis of Viscoelastic Materials," AIAA Journal, Vol. 2, No. 5, May, 1964, pp. 785-808.

APPENDICES

APPENDIX A

NOTATION

APPENDIX A

NOTATION

$A_1, \ldots, A_4$ = constants of integration

$B_1, \ldots, B_4$ = constants of integration

b = member width

$C_1, \ldots, C_4$ = constants of integration

$D(t)$ = creep compliance

D_e = compliance at long time

D_g = compliance at short time

E = modulus of elasticity

$E(t)$ = relaxation modulus

$F(t_k)$ = fictitious equivalent joint load vector

f_k = fictitious distributed load at time t_k

h = length of each element when the member is divided in n-1 equal parts

h = member depth

I = moment of inertia

i = index

K = stiffness matrix

k = constant

k = index

L = member length

M = bending moment

M_k = bending moment at time t_k

M_L = bending moment at left support

M_R = bending moment at right support

m = number of members in a structure

N = axial force

N_k = axial force at a time t_k

n = number of nodes when a member is divided in n-1 equal parts

P = combined joint load vector

$P(t_k)$ = combined joint load vector at time t_k

Q = equivalent joint load vector

$Q(t_k)$ = equivalent joint load vector at time t_k

q = distributed load

q_k = distributed load at time t_k

R = pulley's radius

R_L = transversal reaction at left support

R_R = transversal reaction at right support

r = index

S(t) = time dependent solution

t = time

t_k = a given time

U = member end displacements caused by the combined joint load vector

u = member transversal deflection caused by the combined joint load vector

u_k = u at time t_k

u^I, u^{II}, u^{III}, u^{IV} = first, second, third and fourth derivatives, respectively, of u with respect to the spacial variable x

v = transversal deflection of a member with clamped supports.

v_k = v at time t_k

v^I, v^{II}, v^{III}, v^{IV} = first, second, third and fourth derivatives, respectively, of v with respect to the spacial variable x

W = actual joint load vector

$W(t_k)$ = actual joint load vector at time t_k

X = joint displacement vector

$X(t_k)$ = joint displacement vector at time t_k

x = coordinate along the member axis

Y = member end displacements

Y* = boundary values

y = member transversal deflections under actual loading

y_k = y at time t_k

y^I, y^{II}, y^{III}, y^{IV} = first, second, third and fourth derivatives respectively of y with respect to the spacial variable x

Δ = middle span deflection

$\varepsilon(t)$ = strain as a function of time

ε_o = constant strain

$\sigma(t)$ = stress as a function of time

σ_o = constant stress

τ = time

APPENDIX B

COMPUTER PROGRAMS

APPENDIX B

COMPUTER PROGRAMS

Two computer programs have been written and used for the present study. Program CREEPINV computes Equations (2.21) and (2.22) yielding the values of the relaxation modulus, when the values of the creep compliance are given. Program VIELANAL solves Equation (3.8), giving the deformation history of a plane structure made of linear viscoelastic material. This program uses the subroutine ELASTAN to make an elastic analysis at every fixed time t_k. The listing of this subroutine is omitted, and the reader is referred to reference (18) for a complete description and listing of it.

The important FORTRAN names used in these programs are defined below in alphabetical order. Any name which appears in more than one routine but maintains the same meaning is defined only once.

A(I,J) = coefficients of systems of simultaneous equations

AREA(M) = area of cross section of member M

AXF(M) = axial force in member M

A1(M),..., A4(M) = constants of integration corresponding to member M

B1(M),..., B4(M) = constants of integration corresponding to member M

C1(M),..., C4(M) = constants of integration corresponding to member M

D(KE) = value of creep compliance at time KE

DEL(M) = length of each element into which the member M is divided

E(KE) = value of relaxation modulus at time KE

EAOL(M) = modulus of elasticity times cross section area of member M

EIOL(M) = modulus of elasticity times moment of inertia of cross section of member M

F(M) = axial force in member M

FICT(IX,M,KY) = fictitious load at point IX of member M at cycle KY.

FML(M) = fictitious moment at left end of member M

FMR(M) = fictitious moment at right end of member M

FSL(M) = fictitious shear at left end of member M

FSR(M) = fictitious shear at right end of member M

HO(M) = initial horizontal coordinate of end of member M.

INERT(M) = moment of inertia of member M

K(M) = square root of K2(M)

K2(M) = axial force/fluxural rigidity of member M

K4(M) = square of K2(M)

KE = time

KELIMIT = time limit

KI = iteration number

KY = cycle number

L(M) = length of member M

N = number of nodes on a member divided in N-1 equal parts.

NM = number of members in the structure

NP = total degree of freedom

NPE(M,J) = global degree of freedom of coordinate J of member M

NPR = degree of freedom in rotation

NPS = degree of freedom in linear displacement

P(I) = load at coordinate I of the structure

PFICT(I) = fictitious load at coordinate I of the structure

PP(I) = load at coordinate I of the structure

U(X) = transversal deflection at point x of a member under compression

U4(X) = fourth derivative of U(X)

UU(X) = transversal deflection at point x of a member under tension

UU4(X) = fourth derivative of UU(X)

UUU(X) = transversal deflection at point x of a member under no axial load

V(IX) = transversal deflection at a point IX of a member with clamped ends

V4(IX) = fourth derivative of V(IX)

VO(M) = initial vertical coordinate of end of member M

W(I) = load applied at coordinate I of the structure

X(I) = joint displacement along coordinate I of the structure

XJ(I) = joint displacement along coordinate I of the structure

XLO(M) = initial length of member M

Y(IX) = total transversal displacement at point IX of a member

Y4(IX) = fourth derivative of Y(IX)

Y14(IX,M) = storage of Y4(IX) for use in member M during cycle 1 of new iteration

Y24(IX,M) = storage of Y4(IX) for use in member M during cycle 2 of new iteration

Y34(IX,M) = storage of Y4(IX) for use in member M during cycle 3 of new iteration.

```
      PROGRAM VIELANAL
C=======================================C
C  ANALYSIS OF VISCOELASTIC STRUCTURES  C
C=======================================C
      REAL K,K2,K4,L,INERT
      DIMENSION E(76P)
      DIMENSION PP(20)
      DIMENSION NPE(7,6),HO(7),VO(7),XLO(7),EAOL(7),EIOL(7)
      DIMENSION AREA(7),INERT(7)
      DIMENSION AXF(7)
      DIMENSION XJ(21)
      DIMENSION X(6,7)
      DIMENSION K(7),K2(7),K4(7),L(7)
      DIMENSION W(20)
      DIMENSION Y(10)
      DIMENSION Y4(10)
      DIMENSION FICT(10,7,6)
      DIMENSION DEL(7),F(7)
      DIMENSION A1(7),A2(7),A3(7),A4(7)
      DIMENSION B1(7),B2(7),B3(7),B4(7)
      DIMENSION C1(7),C2(7),C3(7),C4(7)
      DIMENSION PFICT(21),ADUM(20,20),YDUM(20)
      DIMENSION EML(7),EMR(7),ESL(7),ESR(7)
      DIMENSION V(20),V4(20)
      DIMENSION Y14(20,7),Y24(20,7),Y34(20,7)
      COMMON/STRUCT/NP,NPR,NPS,NM
      COMMON/LOAD/PP
      COMMON/MEMBER/MEMNO,NPE,HO,VO,EAOL,EIOL,XLO,L
      COMMON/AXIAL/AXF
      COMMON/JDISPL/XJ
      COMMON/RELAX/F,KELIMIT
      COMMON/TIME/KF
      SINH(X) = 0.5*(EXP(X) - EXP(-X))
      COSH(X) = 0.5*(EXP(X) + EXP(-X))
      U(X)= A1(M)*COS(K(M)*X) + A2(M)*SIN(K(M)*X) +A3(M)*X +
     1      A4(M)
      U4(X) = A1(M)*K4(M)*COS(K(M)*X) + A2(M)*K4(M)*SIN(K(M)*X)
      UU(X) = B1(M)*COSH(K(M)*X) + B2(M)*SINH(K(M)*X) +
     1      B3(M)*X + B4(M)
      UU4(X) = B1(M)*K4(M)*COSH(K(M)*X) + B2(M)*K4(M)*SINH(K(M)*X)
      UUU(X) = C1(M)*X**3/6.0 + C2(M)*X*X*0.5 + C3(M)*X+C4(M)
      READ 10,KELIMIT
  10  FORMAT(I5)
C
      CALL RELAX
C
```

```
C
C  READ AND PRINT STRUCTURE PROPERTIES AND LOADING
C
      READ 20,NP,NPR,NPS,NM
 20   FORMAT(4I5)
      READ 21,(W(I),I=1,NP)
 21   FORMAT(8F10.0)
      PRINT 22,NP,NPR,NPS,NM
 22   FORMAT(///10X,*STRUCTURE PROPERTIES*//
     1      10X,*TOTAL DEGREE OF FREEDOM =*,I3/
     2      10X,*DGR. OF FR. IN ROTATION =*,I3/
     3      10X,*DGR. OF FR. LIN. TRANS. =*,I3/
     4      10X,*NUMBER OF MEMBERS =*,I3//)
      PRINT 23
 23   FORMAT(10X,*EXTERNAL LOADS AT THE JOINTS*/)
      DO 24,I=1,NP
 24   PRINT 25,I,W(I)
 25   FORMAT(19X,*W(*,I3,*) =*,F7.2)
      PRINT 26
 26   FORMAT(//10X,*MEMBERS  PROPERTIES*//10X,
     1      *MEMBER     NP1   NP2   NP3   NP4   NP5   NP6*,9X,
     2      *HO           VO           AREA     MOM. OF INERTIA*/)
      DO 29 I=1,NM
      READ 27, MEMNO,(NPE(I,J),J=1,6),HO(I),VO(I),AREA(I),
     1      INERT(I)
 27   FORMAT(7I5,4F10.0)
      PRINT28,MEMNO,(NPE(I,J),J=1,6),HO(I),VO(I),AREA(I),
     1      INERT(I)
 28   FORMAT(I13,4X,6I5,2X,2F11.2,F13.4,F14.6)
 29   CONTINUE
      READ 30,N
 30   FORMAT(I5)
      PARTS = N-1
      PRINT 31,PARTS
 31   FORMAT(//10X,*EACH MEMBER IS DIVIDED IN*,F5.1,3X,
     1      *EQUAL PARTS*)
      KF =1
      KY = 1
      KI = 0
      EE = E(1)
      DO 32 I=1,NM
      XLO(I) = SQRT((HO(I)*HO(I) + VO(I)*VO(I)))
      L(I) = XLO(I)
      FAOL(I) = EE*AREA(I)/XLO(I)
 32   FIOL(I) = EE*INERT(I)/XLO(I)
      DO 33 I=1,NP
 33   PP(I) = W(I)
C
      CALL ELASTAN
C
```

```
      PRINT 34,KF
 34   FORMAT(1H1,55X,*------------------*/56X,*-*,16X,*-*/
     1      56X,*-    TIME = *,I3,*    -*/56X,*-*,16X,*-*/
     2      56X,*------------------*//)
C
C  PRINT STRUCTURE JOINT DISPLACEMENTS
C
      PRINT 40
 40   FORMAT(//10X,*THE STRUCTURE JOINT DISPLACEMENTS ARE*/)
      DO 41 I=1,NP
 41   PRINT 42,I,XJ(I)
 42   FORMAT(19X,*X(*,I2,*) =*,E13.5)
      PRINT 60
 60   FORMAT(///10X,*TRANSVERSE DEFLECTIONS OF MEMBERS*)
      DO 100 M=1,NM
      DEL(M) = L(M)/PARTS
      F(M) = AXF(M)
      K2(M) = -F(M)/(EE*INERT(M) )
      K4(M) = K2(M)*K2(M)
      K(M) = SQRT(ABS(K2(M)))
C
      CALL UDEFL(X(1,M),F(M),K(M),L(M),A1(M),A2(M),A3(M),
     1      A4(M),B1(M),B2(M),B3(M),B4(M),C1(M),C2(M),C3(M),
     2      C4(M))
C
      IF(F(M) )62,66,64
 62   DO 63 IX=1,N
      SS = IX-1
      XX = SS*DEL(M)
      Y(IX) = U(XX)
 63   Y4(IX) = U4(XX)
      GO TO 68
 64   DO 65 IX=1,N
      SS = IX-1
      XX = SS*DEL(M)
      Y(IX) = UU(XX)
 65   Y4(IX) = UU4(XX)
      GO TO 68
 66   DO 67 IX=1,N
      SS = IX-1
      XX = SS*DEL(M)
      Y(IX) = UUU(XX)
 67   Y4(IX) = 0.0
 68   PRINT 61,M
 61   FORMAT(//10X,*MEMBER*,I2/)
      PRINT 69,((IX,Y(IX)),IX=1,N)
 69   FORMAT(5(5X,*Y(*,I2,*) =*,F13.5))
      DO 100 J=2,6
      J2 = J
      J1 = J-1
```

```
      DO 100 IX=1,N
  100 FICT(IX,M,J) = (F(J2*2**KI)-F(J1*2**KI))*Y4(IX)
     1      / F(1)
  110 IF(KY.LT.6) GO TO 200
      KI = KI + 1
      DO 150 M=1,NM
      DO 142 IX=1,N
  142 Y14(IX,M) = Y24(IX,M)
  150 CONTINUE
      KY = 4
      GO TO 201
  200 KY = KY + 1
  201 KF = KY*2**KI
      EF = F(KF)
      DO 203 I=1,NM
      EAOL(I) = EF*AREA(I)/XLO(I)
  203 EIOL(I) = EF*INERT(I)/XLO(I)
      PRINT 34,KF
      NROW = N-2
      NCOL = N-1
      ITER = 0
  202 DO 220 M=1,NM
C
  220 CALL EQJTLD (FICT(1,M,KY),N,NROW,NCOL,DEL(M),F(M),K2(M),
     1      FML(M),FMR(M),FSL(M),FSR(M),EF,INERT(M),L(M),
     2      ADUM,YDUM)
C
      PFICT(1) = +FMR(1) -FML(2)
      PFICT(2) = FSR(1)
      PFICT(3) = -FSL(2)
      PFICT(4) = +FMR(2) +FML(3)
      PFICT(5) = 0.0
      PFICT(6) = +FSR(2) +FSL(3)
      PFICT(7) = +FMR(3) -FML(4)
      PFICT(8) = FSL(4)
      PFICT(9) = -FSR(3)
      DO 230 I=1,NP
  230 PP(I) = W(I) + PFICT(I)
C
      CALL ELASTAN
C
      DO 240 M=1,NM
      IF( ABS( ABS(F(M)) - ABS(AXF(M)) ) .LT. ABS(0.01*AXF(M)) )
     1      GO TO 240
      DO 241 I=1,NM
  241 F(I) = AXF(I)
      ITER = ITER + 1
      IF(ITER - 50)242,243,243
  242 GO TO 202
  243 PRINT 244,M
```

```
 244  FORMAT(1H1,9X,*AXIAL FORCE IN MEMBER*,I2,
     1       *DOES NOT CONVERGE WITHIN 50 ITERATIONS*)
      GO TO 1000
 240  CONTINUE
      PRINT 229
 229  FORMAT(///10X,*JOINT DISPLACEMENTS*/)
      DO 227 I=1,NP
 227  PRINT 228,I,XJ(I)
 228  FORMAT(15X,*X(*,I2,*) =*,F16.5)
      X(4,1) = X(2,2) = XJ(3)
      X(5,1) = -XJ(2)   $   X(1,2) = XJ(2)
      X(6,1) = X(3,2) = -XJ(1)
      X(4,2) = X(1,3) = XJ(5)
      X(5,2) = X(2,3) = XJ(6)
      X(6,2) = X(3,3) = -XJ(4)
      X(4,3) = X(2,4) = XJ(8)
      X(5,3) = XJ(9)    $    X(1,4) = -XJ(9)
      X(6,3) = X(3,4) = -XJ(7)
C
C  TRANSVERSE DEFLECTIONS  C
C
      PRINT 60
      DO 300 M=1,NM
      F(M) = AXF(M)
      K2(M) = -F(M)/(EE*INERT(M) )
      K4(M) = K2(M)*K2(M)
      K(M) = SQRT(ABS(K2(M)))
C
      CALL UDEFL (X(1,M),F(M),K(M),L(M),A1(M),A2(M),A3(M),
     1       A4(M),B1(M),B2(M),B3(M),B4(M),C1(M),C2(M),C3(M),
     2       C4(M) )
C
C
      CALL VDEFL (FICT(1,M,KY),N,NROW,NCOL,DEL(M),K2(M),
     1       V,V4,A,YDUM)
C
      IF(F(M) )320,324,322
 320  DO 321 IX=1,N
      SS = IX-1
      XX = SS*DEL(M)
      Y(IX) = U(XX) + V(IX)
 321  Y4(IX) = U4(XX) + V4(IX)
      GO TO 326
 322  DO 323 IX=1,N
      SS = IX-1
      XX = SS*DEL(M)
      Y(IX) = UU(XX) + V(IX)
 323  Y4(IX) = UU4(XX) + V4(IX)
      GO TO 326
 324  DO 325 IX=1,N
```

```
      SS = IX-1
      XX = SS*DEL(M)
      Y(IX) = UUU(XX) + V(IX)
  325 Y4(IX) = V4(IX)
  326 PRINT 310,M
  310 FORMAT(//10X,*MEMBER*,I2/)
      PRINT 327,((IX,Y(IX)),IX=1,N)
  327 FORMAT(5(5X,*Y(*,I2,*) =*,F13.5))
      GO TO (340,332,340,334,340,336),KY
  332 DO 333 IX=1,N
  333 Y14(IX,M) = Y4(IX)
      GO TO 340
  334 DO 335 IX=1,N
  335 Y24(IX,M) = Y4(IX)
      GO TO 340
  336 DO 337 IX=1,N
  337 Y34(IX,M) = Y4(IX)
C
C  REDEFINE FICTITIOUS DISTRIBUTED LOADING  C
C
  340 CONTINUE
      JJ = 2
      JY = KY + 1
      DO 299 J=JY,6
      DO 298 IX=1,N
  298 FICT(IX,M,J) = FICT(IX,M,J) +
     1      (F(JJ*2**KI) - F((JJ-1)*2**KI))*Y4(IX)
     2      / F(1)
  299 JJ = JJ+1
  300 CONTINUE
      IF (KF.GE.KELIMIT) GO TO 1000
      GO TO 110
 1000 CONTINUE
      END



      SUBROUTINE RELAX
C
C  THIS SUBROUTINE DEFINES OR READS RELAXATION MODULUS
C
      COMMON/RELAX/F,KELIMIT
      DIMENSION F(768)
C
C  READ RELAXATION MODULUS VALUES
C
      DO 10 I=1,27
      READ 5,K,DUMMY
    5 FORMAT(I5,F10.0)
      E(K) = DUMMY
```

```
 10    CONTINUE
       RETURN
       END



       SUBROUTINE EQUILD (FICT,N,NROW,NCOL,DEL,F,K2,
      1       FML,FMR,FSL,FSR,E,INERT,L,A,Y)
       REAL K2,INERT,L
       DIMENSION FICT(N),A(NROW,NCOL),Y(NROW)
C
C  INITIALIZE
C
       DO 10 I=1,NROW
       DO 10 J=1,NCOL
 10    A(I,J) = 0.0
       C = DEL*DEL*K2
C
C  SQUARE PART OF MATRIX A
C
       N2 = NROW - 2
       N1 = NROW-1
       DO 20 I=1,N2
 20    A(I,I+2) = 1.0
       DO 21 I=3,NROW
 21    A(I,I-2) = 1.0
       DO 22 I=1,N1
 22    A(I,I+1) = C-4.0
       DO 23 I=2,NROW
 23    A(I,I-1) = C-4.0
       DO 24 I=2,N1
 24    A(I,I) = 6.0-2.0*C
       A(1,1) = A(NROW,NROW) = 7.0-2.0*C
C
C  FORM LAST COLUMN OF AUGMENTED MATRIX A
C
       DEL4 = DEL*DEL*DEL*DEL
       DO 30 I=1,NROW
 30    A(I,NCOL) = DEL4*FICT(I+1)
       LL = NROW - 1
C
       CALL SIMEQS(A,NROW,NCOL,LL,Y)
C
       YL2 = (-5.0*Y(1)+4.0*Y(2)-Y(3) )/(DEL*DEL)
       YR2 = (-5.0*Y(NROW)+4.0*Y(NROW-1)-Y(NROW-2) )/(DEL*DEL)
       FML = -F*INERT*YL2
       FMR = -F*INERT*YR2
       SUML = SUMR = 0.0
       DO 40 I=2,NROW
       R1 = I-1
```

```
      SUML = SUML+FICT(I)*DEL*(L-RI*DEL)
 40   SUMR = SUMR+FICT(I)*DEL*(RI*DEL)
      FSL = (-SUML - 0.5*FICT(1)*DEL*(L-DEL*0.25)
     1      -FICT(N)*DEL*DEL*0.125+FML-FMR)/L
      FSR = (-SUMR-0.5*FICT(N)*DEL*(L-DEL*0.25)
     1      -FICT(1)*DEL*DEL*0.125 - FML + FMR) / L
      RETURN
      END



      SUBROUTINE UDEFL(X,F,K,L,A1,A2,A3,A4,B1,B2,B3,B4,
     1      C1,C2,C3,C4)
      REAL K,L
      DIMENSION X(6)
      SINH(X) = 0.5*(EXP(X) - EXP(-X))
      COSH(X) = 0.5*(EXP(X) + EXP(-X))
      IF(F)10,30,20
C
C   MEMBER UNDER COMPRESSION
C
 10   S = SIN(K*L)
      C = COS(K*L)
      D =  (C-1.0)*(K*C-K)+K*S*(S-K*L)
      A1 = ((-X(2)-L*X(3)+X(5))*(K*C-K)-(-X(3)+X(6))*(S-K*L))
     1      /D
      A2 = ((C-1.0)*(-X(3)+X(6))+K*S*(-X(2)-L*X(3)+X(5)))/D
      A3 = X(3)-K*A2
      A4 = X(2) - A1
      RETURN
C
C   MEMBER UNDER TENSION
C
 20   S = SINH(K*L)
      C = COSH(K*L)
      D = (C-1.0)*(K*C-K)-K*S*(S-K*L)
      B1 = ((-X(2)-L*X(3)+X(5))*(K*C-K)-(-X(3)+X(6))*(S-K*L))
     1      /D
      B2 = ((C-1.0)*(-X(3)+X(6))-K*S*(-X(2)-L*X(3)+X(5)))/D
      B3 = X(3) - K*B2
      B4 = X(2) - B1
      RETURN
C
C   MEMBER UNDER NO AXIAL FORCE
C
 30   C1 = (12.0*X(2)+6.0*L*X(3)-12.0*X(5)+6.0*L*X(6))
     1      /(L*L*L)
      C2 = (-6.0*X(2)-4.0*L*X(3)+6.0*X(5)-2.0*L*X(6))/(L*L)
      C3 = X(3)
      C4 = X(2)
```

```
      RETURN
      END


      SUBROUTINE VDEFL (FICT,N,NROW,NCOL,DEL,K2,V,V4,A,Y)
      REAL K2,INERT,L
      DIMENSION FICT(N),A(NROW,NCOL),Y(NROW)
      DIMENSION V(N),V4(N)
C
C   INITIALIZE
C
      DO 10 I=1,NROW
      DO 10 J=1,NCOL
 10   A(I,J) = 0.0
      C = DEL*DEL*K2
C
C   SQUARE PART OF MATRIX A
C
      N2 = NROW - 2
      N1 = NROW-1
      DO 20 I=1,N2
 20   A(I,I+2) = 1.0
      DO 21 I=3,NROW
 21   A(I,I-2) = 1.0
      DO 22 I=1,N1
 22   A(I,I+1) = C-4.0
      DO 23 I=2,NROW
 23   A(I,I-1) = C-4.0
      DO 24 I=2,N1
 24   A(I,I) = 6.0-2.0*C
      A(1,1) = A(NROW,NROW) = 7.0-2.0*C
C
C   FORM LAST COLUMN OF AUGMENTED MATRIX A
C
      DEL4 = DEL*DEL*DEL*DEL
      DO 30 I=1,NROW
 30   A(I,NCOL) = DEL4*FICT(I+1)
      LL = NROW - 1
C
      CALL SIMEQS (A,NROW,NCOL,LL,Y)
C
      V(1) = V(N) = 0.0
      NN = N-1
      DO 40 I=2,NN
 40   V(I) = Y(I-1)
      V4(1) = (-14.0*V(2)+26.0*V(3)-24.0*V(4)+11.0*V(5) -
     1      2.0*V(6) )/DEL4
      V4(N) =(-14.0*V(N-1)+26.0*V(N-2)-24.0*V(N-3) +
     1      11.0*V(N-4)-2.0*V(N-5) )/DEL4
```

```
      V4(2) = (7.0*V(2)-4.0*V(3)+V(4) )/DEL4
      V4(N-1) = (7.0*V(N-1)-4.0*V(N-2)+V(N-3) )/DEL4
      NN = N-2
      DO 50 I=3,NN
   50 V4(I) = (V(I-2)-4.0*V(I-1)+6.0*V(I)-4.0*V(I+1)+V(I+2))
     1      / DEL4
      RETURN
      END



      SUBROUTINE SIMEQS(A,N,M,L,X)
      DIMENSION A(N,M),X(N)
      DO 12 K=1,L
      JJ=K
      BIG=ABS(A(K,K))
      KP1=K+1
C     SEARCH FOR THE LARGEST PIVOTAL ELEMENT
      DO 7 I=KP1,N
      AB=ABS(A(I,K))
      IF (BIG-AB) 6,7,7
    6 BIG=AB
      JJ=I
    7 CONTINUE
      IF (JJ-K) 8,10,8
C     INTERCHANGE ROWS IF NECESSARY
    8 DO 9 J=K,M
      TEMP=A(JJ,J)
      A(JJ,J)=A(K,J)
    9 A(K,J)=TEMP
   10 DO 11 I=KP1,N
      QUOT=A(I,K)/A(K,K)
      DO 11 J=KP1,M
   11 A(I,J)=A(I,J)-QUOT*A(K,J)
      DO 12 I=KP1,N
   12 A(I,K)=0.
      X(N)=A(N,M)/A(N,N)
C     EVALUATE X BY BACK SUBSTITUTION
      DO 14 NN=1,L
      SUM=0.
      I=N-NN
      IP1=I+1
      DO 13 J=IP1,N
   13 SUM=SUM+A(I,J)*X(J)
   14 X(I)=(A(I,M)-SUM)/A(I,I)
      RETURN
      END
```

```
      PROGRAM CREEPINV
C
C  INVERSION OF DISCRETE VALUES OF D(T)
C
      COMMON D(30),E(30),N
      DO 10 I=1,30
 10   READ 11,D(I)
 11   FORMAT(5X,F15.0)
      E(1) = 1.0/D(1)
      E(2)= (1.0-E(1)*(D(2)-D(1))) / D(1)
      E(3)= (1.0 - E(2)*(D(2)-D(1)) - E(1)*(D(3)-D(2))) / D(1)
      N = 30
C
      CALL SOLUTN
C
      PRINT 20
 20   FORMAT(1H1,9X,*TIME              D(T)              E(T)*/
     1     5X,*TENTHS OF MIN.    SQ.IN./LB.       LBS./SQ.IN.*//)
      DO 30 I=1,N
 30   PRINT 31,I,D(I),E(I)
 31   FORMAT(I13,E20.5,F16.5)
      DO 40 I=1,3
      K = 10*I
      D(I) = D(K)
 40   E(I) = E(K)
      DO 41 I=4,6
 41   READ 11,D(I)
      N = 6
C
      CALL SOLUTN
C
      PRINT 50
 50   FORMAT(1H1,9X,*TIME              D(T)              E(T)*/
     1     9X,*MINUTES       SQ.IN./LB.       LBS./SQ.IN.*//)
      DO 51 I=1,6
      PRINT 31,I,D(I),E(I)
 51   PUNCH 52,I,E(I)
 52   FORMAT(I5,F10.1)
      DO 100 I=1,7
      DO 60 K=1,3
      D(K) = D(2*K)
 60   E(K) = E(2*K)
      DO 61 K=4,6
 61   READ 11,D(K)
      N = 6
C
      CALL SOLUTN
C
      DO 62 J=4,6
      KE = J*2**I
```

```
      PRINT 31,KE,D(J),E(J)
62    PUNCH 52,KE,E(J)
100   CONTINUE
      END



      SUBROUTINE SOLUTN
      COMMON D(30),E(30),N
      DO 1001 K=4,N
      SUM = 0.0
      DO 1000 I=2,K
1000  SUM = SUM+E(K-I+1)*(D(I)-D(I-1))
1001  E(K) = (1.0-SUM)/D(1)
      RETURN
      END
```